THE BELL SYSTEM
TECHNICAL JOURNAL

VOLUME XLV SEPTEMBER 1966 NUMBER 7

An Experimental 224 Mb/s Digital Repeatered Line

By I. DORROS, J. M. SIPRESS, and F. D. WALDHAUER

(Manuscript received May 12, 1966)

An experimental digital repeatered line has been developed which transmits information at a rate of 224 Mb/s as part of an experimental high-speed digital transmission system. The PCM terminals and time division multiplex portions were described by J. S. Mayo and others in the November 1965 issue of the Bell System Technical Journal. The repeatered line is described in this paper. The performance of this line is shown to be suitable for coast-to-coast operation.

The line utilizes 0.270-inch copper coaxial transmission lines and regenerative repeaters at one-mile intervals. Ten repeaters have been operated in tandem to form ten miles of repeatered line. Each repeater uses 25 transistors, most of them a new germanium design with a cutoff frequency, f_t, of 4 GHz. Esaki diodes provide the decision thresholds for the regeneration. Power to the repeaters is supplied by dc over the center coaxial conductor. The pulse transmission code is paired selected ternary (PST).

I. INTRODUCTION

Digital transmission of information is becoming increasingly attractive in the telephone plant because it competes favorably both in performance and in cost for telephone service and it allows all kinds of other services such as data and television to share the transmission media with virtually no interaction among the various signals. The digital transmission process[1] is based on (*i*) pulse code modulation of the analog signals to be transmitted, (*ii*) time interleaving of the resultant pulse streams to form a composite pulse stream, and (*iii*) regeneration

in the repeatered line to nullify the effects of noise and distortion encountered in transmission.

The T1 carrier system,[2,3] extremely successful since its introduction in the Bell System in 1962, provided the first wide use of the digital transmission concept. In T1, 24 exchange area voice signals are pulse code modulated, time division multiplexed, and transmitted over cable pairs at a rate of 1.544 megabauds. T1 repeatered lines are now also in use for short-haul data services,[4] since these lines are virtually insensitive to the source of the pulse streams transmitted.

There has also been interest in making use of the features of digital transmission for long-haul transmission. Recently, at Bell Telephone Laboratories, a 224 megabits/second (Mb/s) experimental system was constructed to demonstrate the feasibility of a coast-to-coast system. The PCM terminals and time division multiplex portions of this system were described by J. S. Mayo and others in the November 1965 Bell System Technical Journal.[5,6,7] It was there indicated that the 224 Mb/s information rate would serve either four coded 600 channel mastergroups for a total of 2400 voice channels, 144 T1 signals representing 24 channels each for a total of 3456 voice channels, two coded network TV signals, or some combination of these and other digital signals. In this paper, we describe the experimental repeatered line. The significant accomplishment is the realization of repeater circuits with suitable operating margins that detect and regenerate pulses at a 224 megabaud rate (a baud interval of 4.5 nanoseconds) when each pulse is dispersed by the transmission medium into more than 30 baud intervals and also attenuated to a level limited by thermal noise considerations.

In Section II we give a general description of the line and a summary of performance. In Section III we describe the design of the overall line leading to the requirements on each of the repeaters. The design considerations include the pulse transmission code, the equalization for the loss-frequency characteristic of the coaxial transmission medium and the control of the accumulation of jitter in a chain of repeaters. In Section IV, the design of the repeater is described with emphasis on critical circuits such as the Esaki diode regenerator. Section V reports on performance under laboratory conditions.

II. GENERAL DESCRIPTION

2.1 *Brief Description of the Experimental Repeatered Line*

The configuration of the experimental repeatered line is shown in Fig. 1. The overall performance of such a line is characterized by the

rate of errors introduced into the transmitted stream of information and by the amount of pulse jitter introduced into this stream.

The line operates at error rates below 10^{-10} through ten repeatered links. A coast-to-coast system of about 4000 repeatered links requires an overall error rate below 10^{-6}, or below 2.5×10^{-10} per link. Hence, 4000 mile error performance has been achieved under laboratory conditions.

The pulse jitter measured through ten repeatered links under laboratory conditions was 13 degrees rms. From the model for the accumulation of jitter in a chain of repeaters,[8] this 13 degrees implies that the significant component of jitter introduced *per repeater* is about 3 degrees rms. As will be discussed in Section 3.3.2, 3 degrees is an entirely acceptable performance level in a coast-to-coast system.

An arbitrary stream of binary unipolar pulses from the multiplex at a rate of 223.880 Mb/s is introduced into the line at a binary-to-PST translator as shown in Fig. 1. This translator converts the 2-level pulses into a selected ternary code, called paired selected ternary (PST), for transmission. The details of this code are described in Section 3.1 and also in an earlier paper.[9] Briefly, the ternary transmission of the binary information provides sufficient redundancy (*i*) to allow the transmission of unrestricted binary sequences while still providing timing information to the repeaters, (*ii*) to eliminate dc components from the transmitted spectrum, thus permitting ac coupling in the repeaters and powering at dc, and (*iii*) to allow in-service error monitoring for maintenance purposes.

The ternary signal from the translator has its positive and negative pulses represented as positive pulses on separate leads. These are applied to the transmitting repeater which adjusts levels, combines the two streams, and adds dc power to the signal for serial powering of the repeaters.

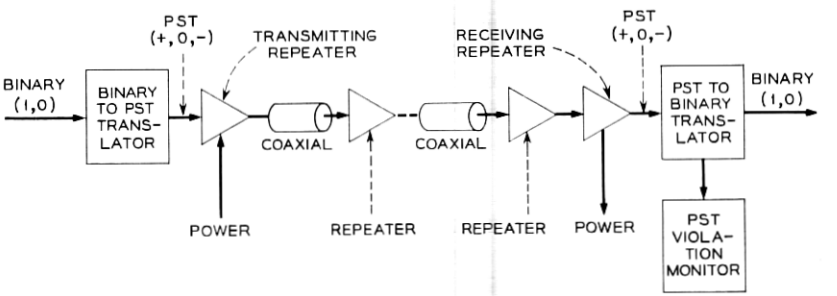

Fig. 1 — Experimental repeatered line.

This system utilizes essentially one mile of an experimental cable with eighteen 0.270-inch coaxials, designed at Bell Laboratories and fabricated at the Western Electric Company's Baltimore Works. The cable design will be reported on separately. Each repeatered link uses one of the 18 coaxials in the cable. Electrically, the coaxial line inserts a loss that is proportional in dB to the square root of frequency ($\sqrt{f}$) over the frequency range of interest. At a nominal temperature, the loss of a mile of 0.270-inch coaxial line is 57 dB at 112 MHz, one-half the baud rate. The propagation characteristics of the experimental cable are essentially equivalent to those of standard Bell System coaxial cables used for L-carrier transmission.[10] Hence, the spacing of the repeaters on the 0.375-inch standard coaxials now generally being installed would be that of the experimental system modified by the ratio of the diameters [(1.0 miles) $\times$ (0.375/0.270) = 1.4 miles].

The regenerative repeater, of the forward acting complete retiming variety,[11] performs the three R's — reshaping, retiming, and regeneration. To reshape, an equalizer compensates for the $\sqrt{f}$ propagation characteristic of the transmission medium in such a manner as to compromise among the intersymbol interference, the noise entering at the repeater preamplifier, and other important degrading effects. The repeater spacing is controlled by this compromise. To retime, a sine wave with average frequency equal to the baud rate is extracted from the pulse train by nonlinear means. This sine wave in turn generates regularly spaced pulses of short duration for sampling the equalized waveform. To regenerate, a 3-level decision is made at each sampling instant to determine whether a +, 0, or − pulse is to be emitted in each baud interval. A detailed description of the repeater is given in Section IV.

In the experimental system, 10 such repeatered links have been operated in tandem, looping through 10 coaxials of the 18-coaxial cable to form 10 miles of line.

In the receiving repeater, the dc powering circuit is completed, the levels are adjusted, and the positive and negative pulses are separated into two unipolar streams for application to the PST-to-binary translator. Finally, a PST violation monitor makes use of a redundant property of the PST code to monitor errors as described in Section 3.1.4.[9]

2.2 *Main Stations*

An actual long-haul repeatered line would have main stations spaced at appropriate intervals to house equipment for (*i*) powering the line repeaters through the transmitting and receiving repeaters, (*ii*) isolating and automatically switching out a section of line for maintenance pur-

poses, (*iii*) controlling the accumulation of pulse jitter in a long repeatered line,[5,7] and (*iv*) dropping and adding information-bearing pulse streams (multiplexing).

The main station spacing appears to be determined primarily by the multiplexing considerations. The limitation due to powering is based on the power required by the repeaters and the maximum practical voltage which can be applied to the coaxials and the repeaters. The limitation due to section isolation considerations depends on the combined reliability of the cable and the repeaters. We will not deal with the power and section isolation questions in this paper, but we will show in Section 3.3 that jitter control is required only at very distant spacings, and hence is not a consideration in the spacing of main stations.

III. DESIGN OF THE LINE

The overall design of the experimental 224 Mb/s digital repeatered line is described in this section; the repeater itself is described in Section IV. We discuss the pulse transmission code in Section 3.1, the equalization of a link of repeatered line in Section 3.2, and the retiming of such a link in Section 3.3. The derivation of performance objectives for a single repeater from the overall objectives for a 4000-mile system is included; we treat error rate in Section 3.2 and jitter in Section 3.3.

3.1 *Pulse Transmission Code*

3.1.1 *Purposes of a Transmission Code*

The binary information from the multiplex must be coded into a sequence of signal symbols that is readily transmitted over a practical line. The transmission code adds redundancy to the binary information to permit the three specific functions described below.

Conceptually, the simplest pulse transmission code is unipolar in which the binary marks and spaces are coded for transmission as presence and absence of pulses. There are three significant practical problems associated with this unipolar format:

(*i*) Timing information must be extracted from the pulse train at each repeater to determine when the pulse, no-pulse decisions should be made and to retime the regenerated pulses emitted by each repeater. Long sequences of binary spaces result in long periods without pulses and hence, without timing information. This in turn yields poor timing performance, leading to increased error rate and pulse position jitter.

(*ii*) Since the repeaters are serially powered by means of dc trans-

mitted on the center conductors of the coaxials, the signal path in the repeaters cannot be dc coupled to the cable medium. Consequently, the transmission of varying densities of marks results in dc wander of the pulse stream, thereby reducing drastically the margins in the detection process. DC restoration circuits which could eliminate this wander appeared unfeasible for the experimental repeater because of the high baud rate.

(*iii*) Some method of determining error performance without the interruption of service is essential for maintenance purposes. In-service monitoring of the line error rate with the unipolar format as described above is impossible because each unipolar binary symbol carries exactly 1 bit of information with no redundancy.

All three of these problems can be eliminated by introducing redundancy into the coding process. In the experimental line, the required redundancy is obtained by employing 3-level transmission (+,0,−) at a line baud rate equal to that of the binary information rate. This redundancy is $\log_2 3 - 1 = 0.59$ bits/symbol.

Another means of achieving the necessary redundancy is to utilize polar binary transmission at a line baud rate higher than the information rate. This appears to be an unattractive alternative for a coaxial medium because the higher baud rate, resulting from a compromise satisfying the above three constraints with reasonable coding complexity, more than offsets the potential signal-to-noise advantage of detecting 2-level signals rather than 3-level signals.

3.1.2 *The Paired Selected Ternary (PST) Code*

The pulse transmission code is paired selected ternary (PST).[9] In this code, the binary sequence to be transmitted is framed into pairs and translated into a ternary format according to Table I. There are two modes in the PST code and the mode is changed after each occurrence of either a 10 or a 01 binary pair. As an example of PST coding, consider the following binary sequence and the corresponding PST sequence.

BINARY	10	01	00	01	11	01
PST	+0	0−	−+	0+	+−	0−

Note the change of mode after each occurrence of a 10 or a 01 pair in the binary sequence.

Six of the nine possible ternary symbol pairs are used to represent the four possible binary symbol pairs. The remaining three unused ternary symbol pairs are used for framing the pairs at the receiver.

TABLE I—THE PAIRED SELECTED TERNARY CODE

Binary	PST	
	+ Mode	− Mode
11	+−	+−
10	+0	−0
01	0+	0−
00	−+	−+

Change mode after each 10 or 01

The alternation of modes produces a null in the power spectrum at dc when the positive and negative pulses are balanced (identical except for sign). This enables dc powering of the repeaters. The PST power spectrum, $W(f)$, normalized to the baud interval, T, is presented in Fig. 2 for the case of equally likely marks and spaces in the original binary sequence [$p(1) = p(0)$], cosine-squared pulses one baud interval in duration at the base, and balanced positive and negative pulses. For other than this idealized situation, see Ref. 9.

The coding of the 00 binary pair into the −+ PST pair eliminates the timing problems associated with the transmission of long sequences of 0's. An additional feature of the PST code is that timing information

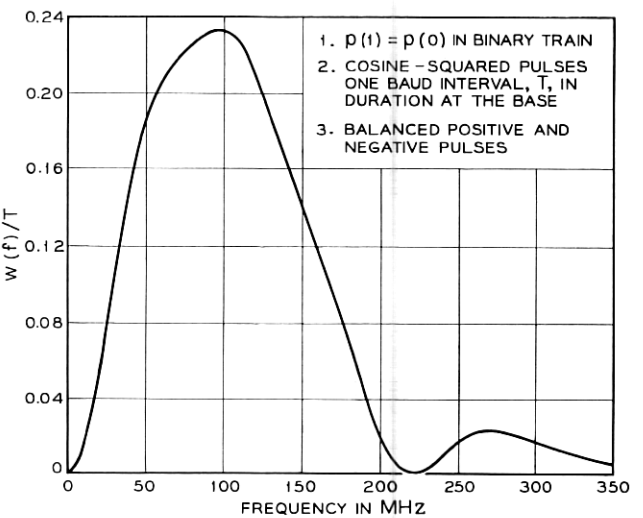

Fig. 2 — PST power spectrum for a random binary sequence.

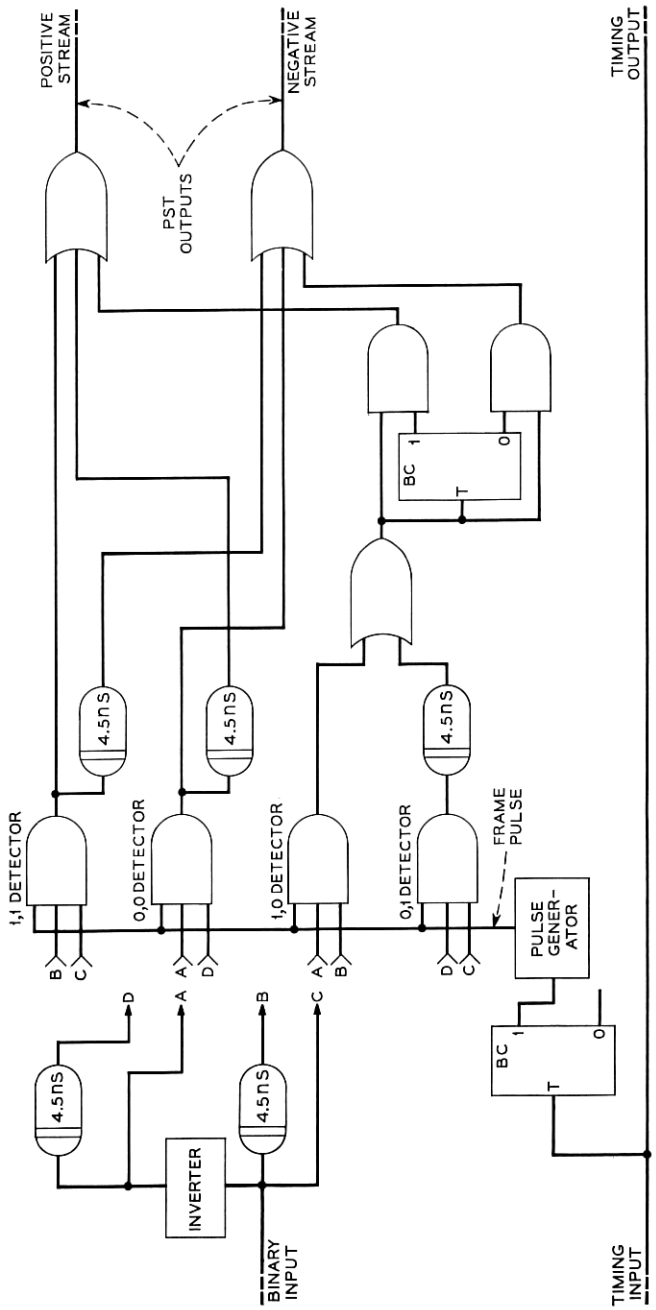

Fig. 3 — Logical diagram of the binary-to-PST translator.

at the repeaters can be extracted by nonlinear means (rectification). This avoids the harmonic and phase distortion problems associated with other schemes involving the linear extraction of timing information from the low-level components received at the baud frequency.

A logical diagram of the binary-to-PST translator is shown in Fig. 3.

3.1.3 *Translation of PST Sequences Back Into Binary*

At the receiving end of the line, the original binary sequence is recovered from the selected ternary sequence in the PST-to-binary translator.

Framing is essential to associate the symbols which are part of the same PST pair. The effect of incorrect framing is demonstrated below.

Binary		1 0		0 1		0 0		0 1		1 1		0 1		
PST		+0		0−		−+		0+		+−		0−		
Incorrectly framed PST	+		0 0		−−		+0		++		−0		−	
Incorrect binary			?		?		1 0		?		1 0			

The unused $++$, $--$, and 00 ternary pairs are detected to indicate an out-of-frame condition.

The PST-to-binary translator is shown in Fig. 4. Out-of-frame indications are applied to a flywheel circuit which prevents randomly occurring line errors from initiating a change in frame. The flywheel requires that three out-of-frame indications occur within 19 consecutive pairs (38 baud intervals or 170 nanoseconds) to initiate a change in frame. The cumulative probability of obtaining three out-of-frame indications within J consecutive pairs after going out of frame is given by the $N = 3$ curve in Fig. 5 for the case of equally likely marks and spaces in the original binary sequence. The mean time (in PST pairs) to occurrence of N out-of-frame indications is shown as M.

To reduce the effect of erroneous frame shifts due to line errors, the flywheel is disabled for a period of 19 pairs after a change in frame. During this period, only one out-of-frame indication is required to initiate a second frame shift pulse, thereby reestablishing the original framing condition. The cumulative probability of obtaining one out-of-frame indication within J pairs is indicated by the $N = 1$ curve in Fig. 5. The mean time to an incorrect initiation of a change of frame due to randomly occurring line errors is shown in Fig. 6 as a function of error rate, assuming $p(1) = p(0) = \frac{1}{2}$. For the required error rates of 10^{-6}, such false misframes are extremely unlikely.

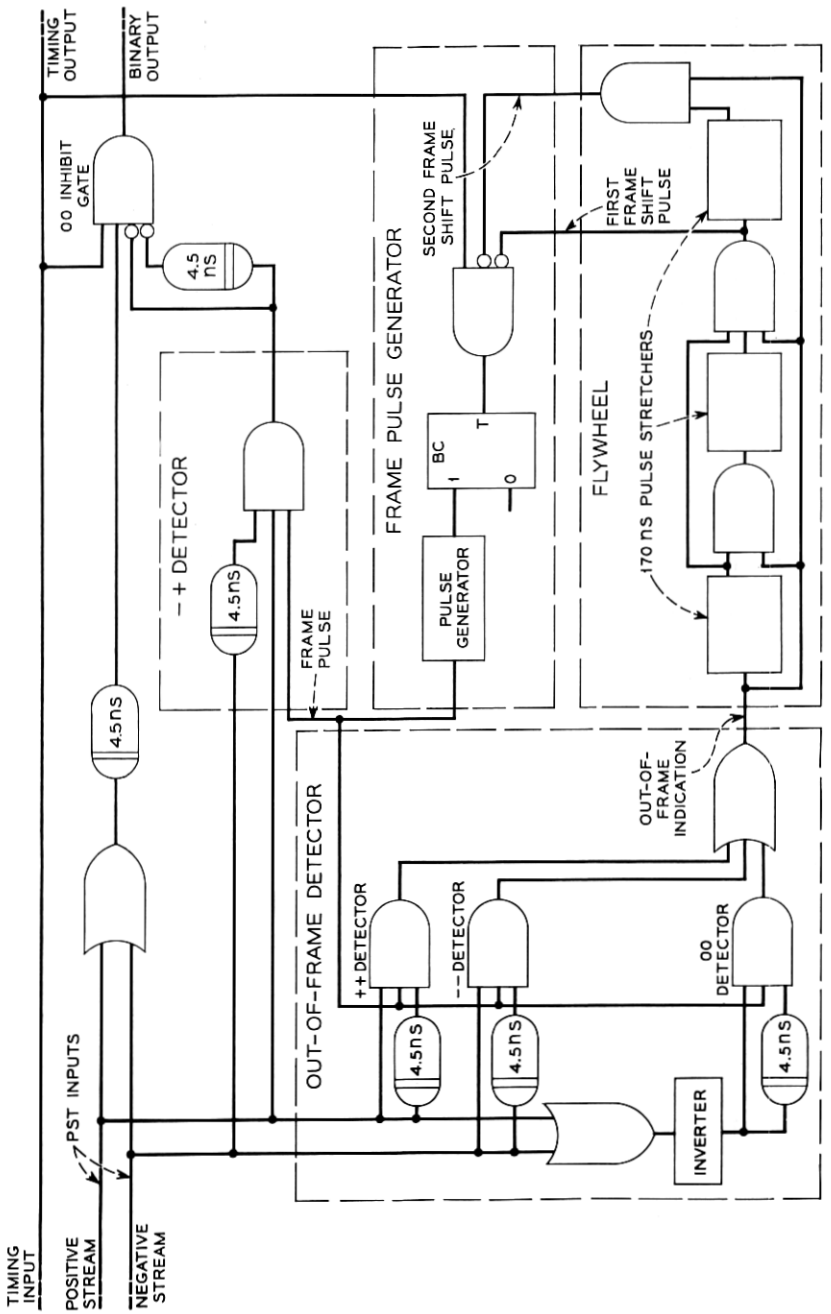

Fig. 4 — Logical diagram of the PST-to-binary translator.

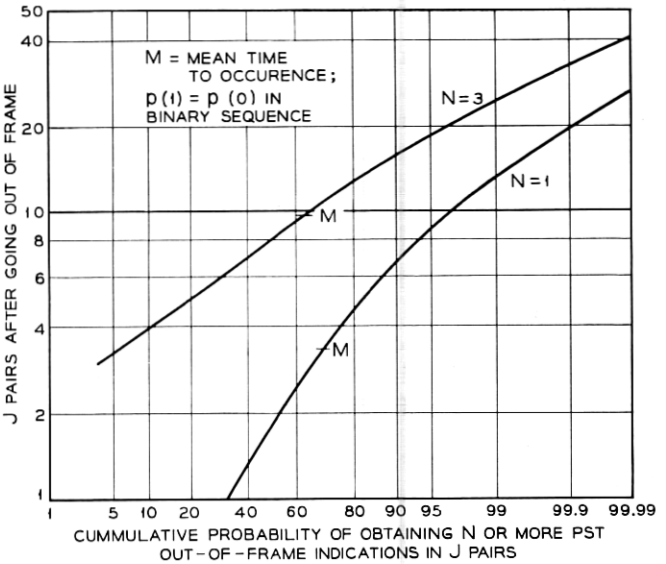

Fig. 5 — Probability of obtaining N or more PST out-of-frame indications in J pairs.

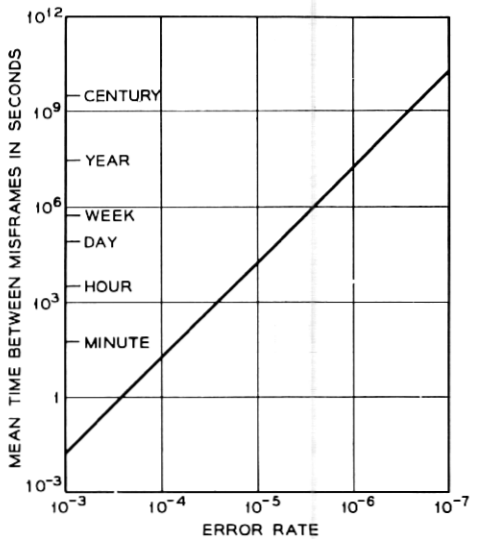

Fig. 6 — Misframes due to random line errors.

3.1.4 *In-Service Error Performance Monitoring*

A method of monitoring line error performance without interrupting service is a necessary maintenance feature of a long-haul digital transmission system. PST sequences contain certain properties which are violated only when errors occur. Violations of these properties can be monitored to determine the error performance on an in-service basis.

Four different properties whose violation provide means of error monitoring are given in Ref. 9. One of these, the *bipolar property* of PST, is employed in the experimental line.

To error monitor with the bipolar property, we first remove all of the $+-$ and $-+$ ternary pairs from the pulse stream. The remaining pulses, which come from coding the binary 10 and 01 pairs, alternate in polarity. An error causes a violation of this alternation or bipolar property, as in the example below.

PST pulse stream	$+0 \quad 0- \quad -+ \quad 0+ \quad +- \quad 0-$
PST with $+-$ and $-+$ removed	$+0 \quad 0- \quad 0\,0 \quad 0+ \quad 0\,0 \quad 0-$
	Error ↓
PST with error	$+0 \quad +- \quad -+ \quad 0+ \quad +- \quad 0-$
	Violation ↓
PST with error and $+-$ and $-+$ removed	$+0 \quad 0\,0 \quad 0\,0 \quad 0+ \quad 0\,0 \quad 0-$

The violation can occur some time after the error, but all singly occurring errors* are detected.

A logical diagram of the PST violation monitor is shown in Fig. 7.

Since this form of violation monitoring requires framing common to PST-to-binary translation, these two functions have been combined in one circuit in the experimental system.

3.1.5 *Circuit Techniques for PST Code Translation*

The laboratory realization of the PST code translation equipment has made extensive use of Schottky barrier diodes and emitter-coupled current-routing pairs using transistors having an f_T of 3 GHz. The diodes perform the logic and the current routing pairs provide isolation, amplification, amplitude regeneration, and, when appropriately connected, logical inversion. Fig. 8 shows one of the four binary pair detectors in the

* For the low error rates we are interested in, the rate of singly occurring errors is essentially the total error rate.

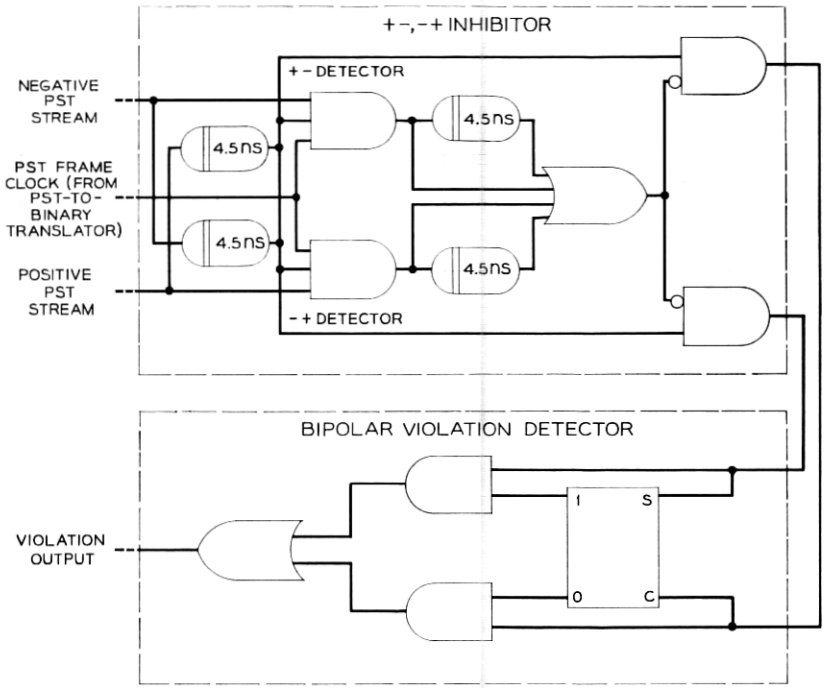

Fig. 7 — Logical diagram of the PST violation monitor.

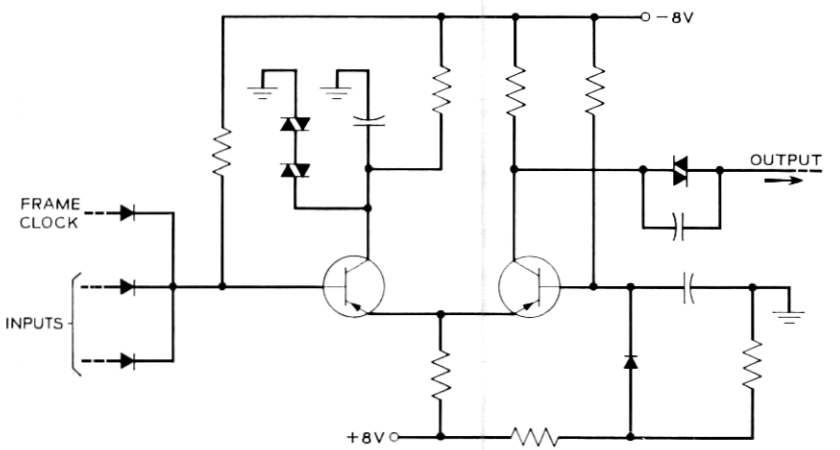

Fig. 8 — Binary pair detector at the input of the PST-to-binary translator — typical of the logic gates in the code conversion equipment.

binary-to-PST translator, a circuit typical of the logic gates used throughout the translation equipment. The input signals to the gates are at least one-half volt to insure complete switching of the emitter current from one transistor to the other.

Another circuit used extensively in the code translation equipment is the Goto pair binary counter, shown in Fig. 9, which employs two Esaki diodes.

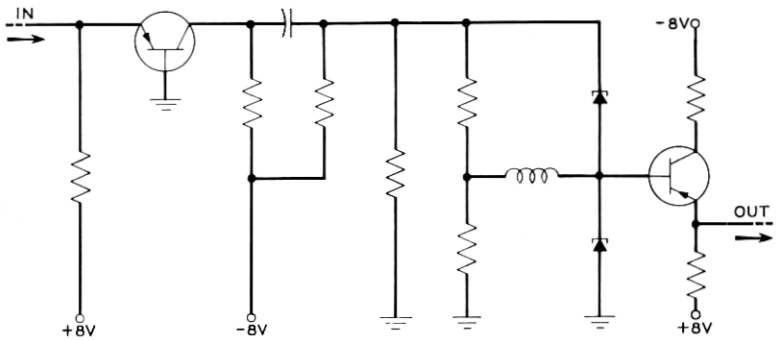

Fig. 9 — Goto pair binary counter using two Esaki diodes.

3.2 *Equalization of a Link of the Repeatered Line*

3.2.1 *The Error Rate Objective*

The preliminary overall error rate objective for a 4000-mile digital repeatered line is a maximum of 10^{-6}, based upon subjective testing and computation of noise power in the terminal signals due to line errors. Such an error rate will introduce negligible degradation into analog signals arising from services such as message, television, *Picturephone** and voiceband data, and will yield high performance for signals already in digital form such as computer outputs.[12] If we assume an approximate repeater spacing of one mile, we obtain a maximum error rate objective of 2.5×10^{-10} per repeatered link, or approximately 10^{-10}. This calculation assumes uniform operation of all repeaters. In a field situation, we would expect to permit somewhat poorer performance in several repeaters since the bulk of the repeaters normally would be operating at substantially better than this level. To place an objective on this, however, requires more knowledge of uniformity of repeater operation than is presently available.

* Service mark of the Bell System.

3.2.2 *Model of the Signal Path*

A model of the signal path in a link of a repeatered line is shown in Fig. 10. The signal path begins at the regenerator output in a repeater and ends at the regenerator input in the next repeater. The overall transmission of the signal path from $S_N(f)$ to $R_N(f)$ is denoted $T(f)$.

The loss of a coaxial tube in a cable, $C(f)$, is primarily dependent on the skin effect in the conductors and therefore this loss in dB is essentially proportional to the square root of frequency in the range of interest to us, and linearly proportional to the cable length. A single pulse through $C(f)$ alone is highly attenuated and severely dispersed and therefore gain and equalization are required to amplify and shape the pulse stream prior to detection in the regenerator. In the model, there are two equalizing blocks, $E_1(f)$ and $E_2(f)$, and two amplifying blocks, $A_1(f)$ and $A_2(f)$. The details of this separation will be discussed later, but it can briefly be stated here that the amplifier split is to sectionalize the required high gain, and the equalizer split is a compromise to limit the noise bandwidth, to prevent overload of the preamplifier, and to provide surge protection for the repeater output. The power separation filters at the input and output of the repeater are included in $A_1(f)$ and $E_1(f)$.

Our analyses have been carried out with cosine-squared regenerator output pulses one-half baud interval in duration at half-amplitude. This is a good approximation for the experimental system. The detailed shape of these pulses is not important because the spectrum of such a narrow pulse is nearly flat over the important frequencies in $T(f)$, which only go up to about three-fourths of the baud frequency. Hence, it is

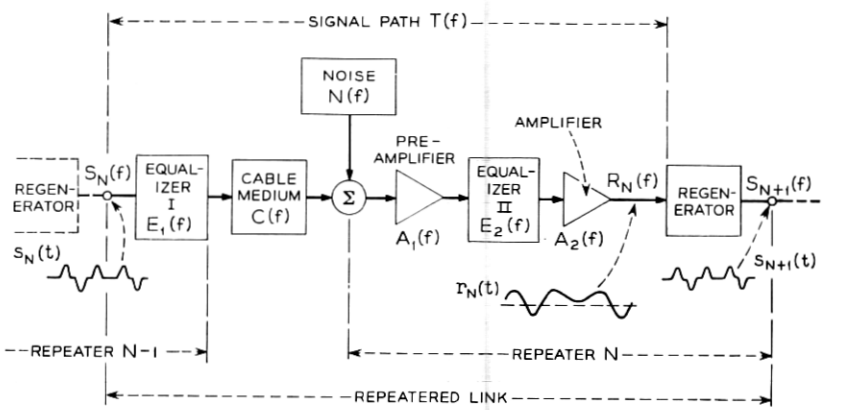

Fig. 10 — Signal path model.

only the total *area* of these pulses that is important. The pulse duration used was chosen for convenience in implementation.

The outer conductor of the coaxial is 0.005-inch thick copper with a soldered seam. The conductor thickness is sufficient to essentially isolate the signals inside the coaxial from the outside world. Hence, the controlling disturbance to the signal is the sum of the thermal noise of the cable and the noise generated in the preamplifier. This is shown in the model as an equivalent noise source at the preamplifier input, $N(f)$.

The key measure of the performance of a repeater is the error rate. This rate, in turn, is dependent on the ability of the regenerator to decide correctly whether +, 0, or − pulses were transmitted in each of the baud intervals. We are, therefore, highly concerned about the details of the waveform at the regenerator input, $r_N(t)$. Equalization $E_1(f)E_2(f)$ compensates for the shape of $C(f)$ and the imperfections in the transmission characteristic of $A_1(f)A_2(f)$. Also, the bandwidth of the noise entering the regenerator is primarily determined by $E_2(f)$. The optimum equalization maximizes the repeater spacing for a given error rate objective by means of a compromise between intersymbol interference and noise, while taking into account variations in coaxial loss due to temperature variations, sampling amplitude threshold offset, sampling timing misalignment, and other practical degradations.

An analytical solution for the optimum equalization in the face of all of the practical degradations in the repeatered link is not tractable. The general problem of optimum equalization for pulse detection has been treated in the literature,[13,14] but nowhere, including in analyses of our own, is there a solution to an applicable model. Consequently, we simulated the repeatered link on a digital computer in such a manner as to allow examination of the effects of the following:

(*i*) variations in the transmission characteristics of the coaxial, $C(f)$, the amplifiers, $A_1(f)$ and $A_2(f)$, and the equalizers, $E_1(f)$ and $E_2(f)$;
(*ii*) Gaussian noise with arbitrary power spectrum;
(*iii*) static and dynamic sampling time misalignment;
(*iv*) variations in detection threshold;
(*v*) variations in the statistics of the input binary sequence;
(*vi*) variations in the regenerator output pulse shape.

3.2.3 *Signal-to-Noise Ratio and Error Rate*

The theoretical error rate in the detection of a signal in the presence of Gaussian noise follows the well-known curve shown in Fig. 11.[15] Note that we have plotted peak signal-to-rms-noise. It is the *peak* signal that is of interest to us since the power limitation is in the repeater

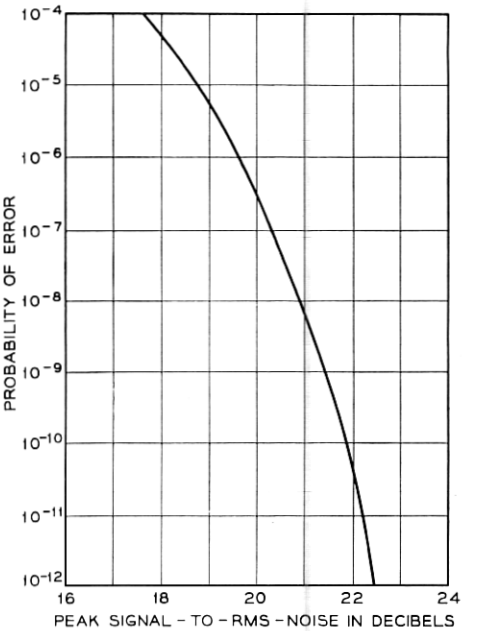

Fig. 11 — Theoretical error rate as a function of peak signal-to-rms-noise ratio.

peak output capability, not in its average signal power. Also, because of the shielded nature of the coaxial medium, transmitted signals do not interfere with any other signals.

The interpretation of Fig. 11 is that the average error rate indicated by the ordinate will prevail if the ratio of the peak of an isolated pulse to rms Gaussian noise, with no interfering signals or other degrading effects at the time of detection, is the quantity in dB indicated by the abscissa. Under practical conditions with a high baud rate there *will* be intersymbol interference and other degradations. Hence, at the decision instants the signal will depart from the ideal case, where there is either a full peak or no signal at all, and where the decision time instant and threshold are perfect. Fig. 11 must, therefore, be interpreted appropriately.

To avoid the difficulty of dealing with statistical intersymbol interference and other degradations, we conservatively design for the worst case. Hence, Fig. 11 may be used to determine the upper bound on the error rate if the *peak signal* is interpreted as the difference at the sampling instant between the minimum amplitude of all received pulse signals and the maximum amplitude of all received no-pulse signals.

The worst case is the combination of the worst intersymbol interference resulting principally from cable temperature changes and circuit imperfections, and the other degradations such as nonideal sampling where both the time instant and the threshold are imperfect. The lumping of the other degradations with intersymbol interference is illustrated in Fig. 12 using the ternary eye. This eye represents the inner boundaries of all possible pulse sequences superimposed and synchronized with the baud rate; in addition, the boundaries have been displaced inward vertically and horizontally to account for the other degradations. Resulting eye heights H_+ and H_- now represent the peak signal for use on Fig. 11, and the time and amplitude crosshairs now are of zero width. In what follows, H is taken to represent either H_+ or H_-.

From Fig. 11, we see that in order to maintain the per repeater 10^{-10} error rate objective indicated in Section 3.2.1, under extreme conditions (due to pulse sequences, cable temperature, parameter drifts, and sampling time and threshold displacements), the ratio of H to the rms noise must be 22 dB. It follows then that the ratio of the peak of the pulse, P, to the rms noise is greater than the theoretical value of 22 dB by an impairment defined as

$$I = 20 \log (P/H).$$

The impairment, I, is the excess peak-signal-to-rms-noise ratio in dB required to compensate for the worst case degraded eye due to the total of the intersymbol interference and other degradations. Due to the rapid increase with frequency of the loss of the coaxial, a small increase in equalized bandwidth for the purpose of reducing intersymbol interference produces a large increase in noise. The compromise between intersymbol interference and noise, therefore, is balanced in favor of reduced bandwidth. Our specific compromise allows enough intersymbol interference and other degradations to reduce H to 0.2 P, which corresponds to an I of 14 dB.

It should be pointed out that the eye opening, H, is an artificial one with idealized crosshairs and, therefore, is not what is seen on an oscilloscope at the regenerator input. What is seen on an oscilloscope is the eye with all degradations up to the input to the practical detector. The detector, however, has its own degradations which *are* included in the artificial eye.

3.2.4 *Signal Path Parameters for the Experimental Line*

The digital computer simulation and actual circuit performance achievements have led to the signal path parameters of Table II for a

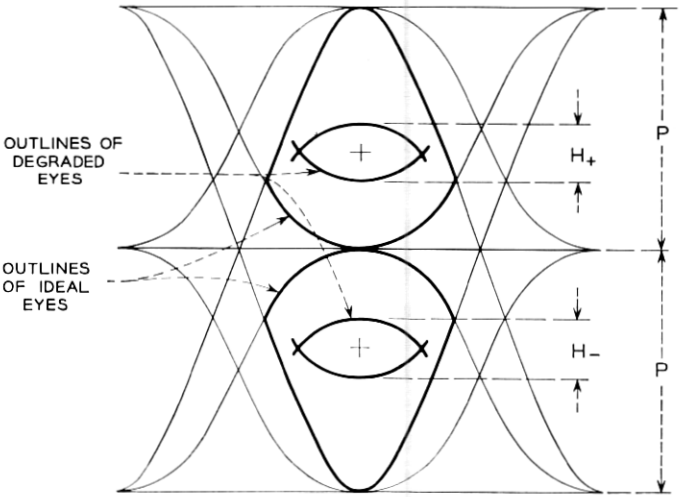

Fig. 12 — Ideal and degraded eyes.

repeatered link. These parameters have been realized, but under laboratory degraded conditions rather than worse case conditions.

Table III gives an example of the extreme conditions simultaneously permitted by the design implied by Table II.

The signal path parameters of Table II impose the requirements on the design of the repeater itself, to be discussed in detail in Section IV. For the present, we have specified, (*i*) the loss of the cable at the half

TABLE II — SIGNAL PATH PARAMETERS OF A REPEATERED LINK

Worst case error rate		10^{-10}
Repeater peak output power		+14 dBm
Preamplifier noise figure		6 dB
Theoretical peak signal-to-rms-noise ratio for 10^{-10} error rate		22 dB
Impairment, I, for worst case degradations		14 dB
Ratio of peak equalized single pulse to rms noise under nominal conditions		36 dB
Loss of coaxial between repeaters (Corresponding length of 0.270-inch coaxial at nominal 55°F)		57 dB at 112 MHz (5320 ft)
Equalizer singularities	Zeros:	11 MHz 15 MHz 70 MHz
	Poles:	94 MHz 161 MHz $\angle \pm 117°$ 196 MHz $\angle \pm 114°$

TABLE III — EXAMPLE OF EXTREME CONDITIONS SIMULTANEOUSLY PERMITTED

Cable temperature rise	21°F (maximum expected)
Equivalent echo at the sampling instant	20% of the pulse peak
Sampling amplitude threshold offset	10% of the pulse peak
Static sampling timing misalignment*	20°
Dynamic sampling timing misalignment distribution*	$\cos^4$ with 60° base width
Noise figure	7 dB

* 360° is one baud interval.

baud rate which bears on the gain in the repeater,† (*ii*) the required output power and noise figure of the repeater, (*iii*) the equalizer singularities, and (*iv*) the allowed impairment. The repeater design will take up from there.

As an indication of the significance of these signal path parameters, we refer to Figs. 13 through 17. First, the loss at 55°F of a coaxial be-

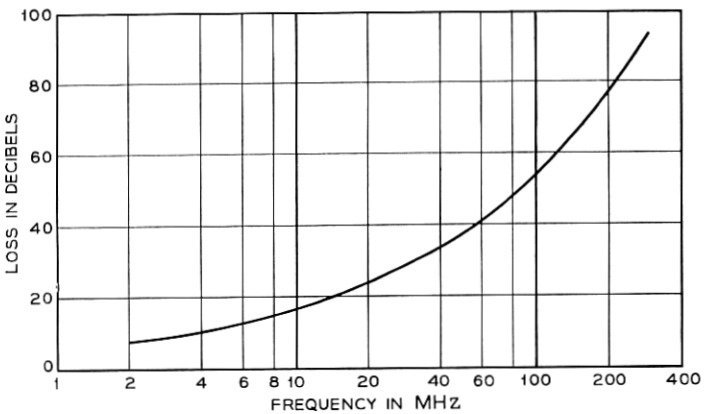

Fig. 13 — Loss of 5320 feet of 0.270-inch coaxial at 55°F on the usual log f scale.

tween repeaters is shown in Fig. 13 plotted on the usual log frequency scale in accordance with conventional characterization of transmission media. This curve (loss in dB) follows essentially the square root of frequency and goes through 57 dB at 112 MHz.

The nominal losses of the cable, the equalization including the effect of the amplifiers, and the overall channel with 50 dB net effective flat gain, are shown in Fig. 14.

† The loss of the peak of a pulse through the signal path is given approximately by the loss of this path at a frequency corresponding to half the baud rate.[16]

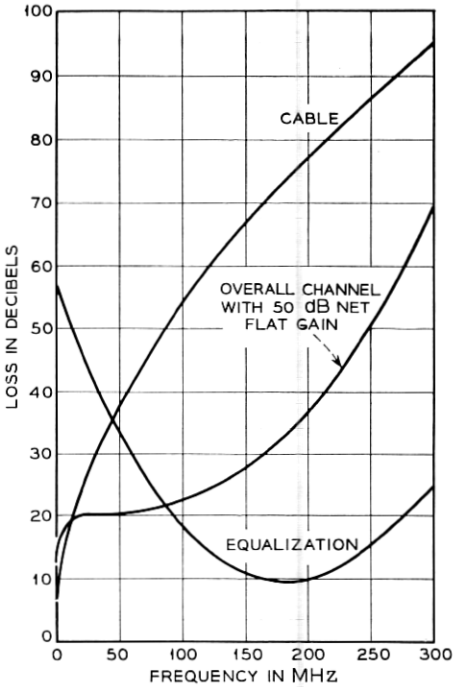

Fig. 14 — Cable, equalization, and overall channel loss characteristics.

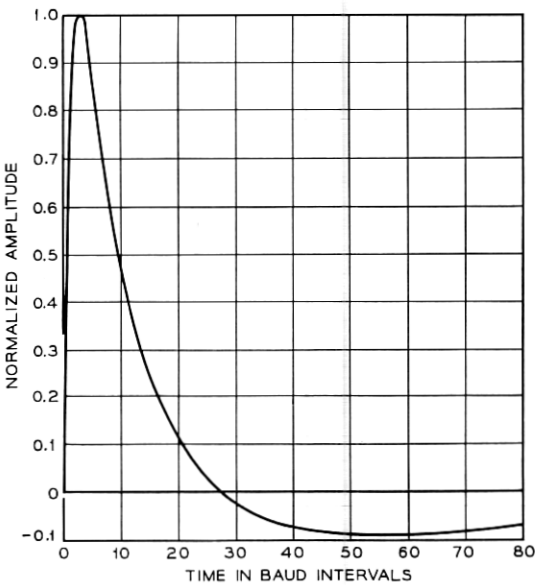

Fig. 15 — Nominal isolated pulse without equalization.

Due to the great variation of the cable loss over the frequency band of interest, the nominal isolated pulse without benefit of equalization is severely dispersed as shown, normalized to its own peak, in Fig. 15. It has a rise time of about 3 baud intervals and a fall time of about 25 baud intervals. The undershoot is due to the lack of dc transmission in the power separation filters and is of little significance since there are balanced numbers of positive and negative pulses in the PST code. As a result of the dispersion, the peak amplitude of all possible unequalized pulse sequences varies over a 28-dB range. The problem of dealing with the resulting large dynamic range in the repeater is discussed further in Section 4.1.

The nominal single equalized pulse is shown in Fig. 16. It is apparent that the amplitudes at -1.0, $+1.0$, $+2.0$, and $+3.0$ baud intervals are small. Under degraded conditions, however, these amplitudes are substantial. The low amplitude negative tail of such an isolated pulse, which obviously must be present in the response of a channel without dc transmission, is off the chart. The inner boundary of the superposition of this single pulse in all possible PST sequences forms the nominal eye shown in Fig. 17. The uppermost curve in this figure is the envelope of the maximum values of all pulse sequences. The slow-acting automatic

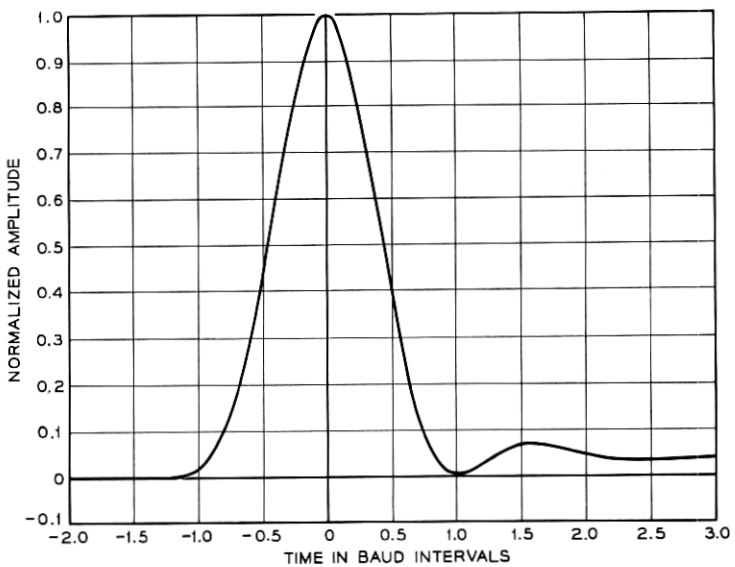

Fig. 16 — Nominal single equalized pulse.

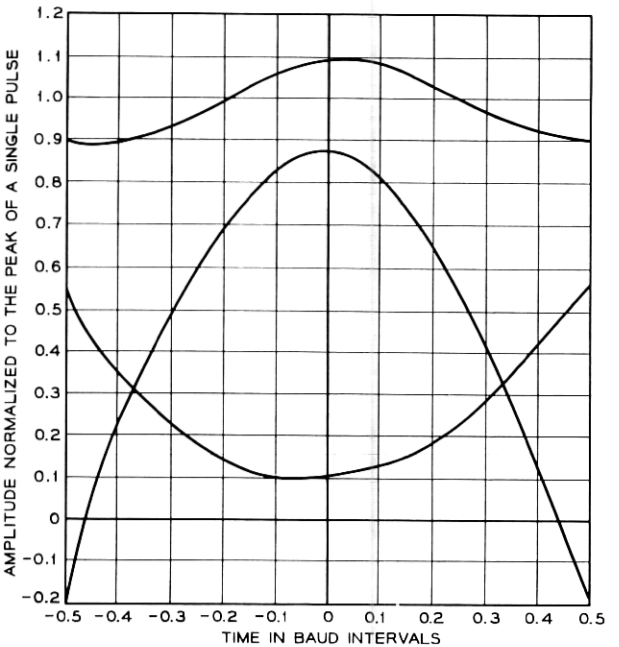

Fig. 17 — Nominal positive eye at the regenerator — inner boundary of the superposition of all possible PST sequences using the nominal single equalized pulse shown in Fig. 16.

gain control (AGC) in the repeater operates substantially on the peak of this curve. It should be emphasized that this nominal eye is the one seen on an oscilloscope and does not include the effects of the finite crosshair widths.

3.3 *Retiming in the Repeatered Line*

3.3.1 *Timing Extraction at Each Repeater*

The function of the repeater timing path is to extract timing information from the equalized ternary pulse stream. As discussed previously, this timing information is used to determine when the pulse, no-pulse decisions should be made as well as to retime the pulses transmitted from the repeater.

The repeater uses forward acting complete retiming[11] with nonlinear extraction of the timing component from the PST sequence. The equalized pulse stream is full-wave rectified and the upper portion of the

resulting unipolar stream is amplified and applied to a simple tuned circuit. The output of this is amplified and limited to produce a constant amplitude sinusoid which, in turn, drives a timing pulse generator.

Each repeater introduces phase variation, or timing noise, called jitter, into the extracted timing information. This jitter contains a systematic component which is a function of the transmitted pulse pattern and accumulates in a chain of repeaters considerably faster than the pattern independent, nonsystematic component.

The amounts of jitter introduced in and transmitted through each repeater can be kept low by a small effective bandwidth in the timing path. The smaller this bandwidth, however, the larger the static sampling timing misalignment for a given and inevitable mistuning of the timing extraction circuit.

The jitter accumulation and the objective for the jitter introduced in each repeater are discussed next.

3.3.2 *Control of Jitter Accumulation and the Requirements on a Single Repeater*

The preliminary objective for band-limited jitter at the end of a 4000-mile line is as shown in Fig. 18. This was derived on the basis of coded mastergroup message service in which the top frequency is 2.788 MHz, such as in an L600 mastergroup or a U600 mastergroup shifted down in frequency for more efficient sampling.* Based upon preliminary analysis and subjective testing, however, this objective is probably controlling for all digital and analog type services including data and network television. These two latter services, however, require further study.[12] The effect of low-frequency jitter within the objective shown is a signal-to-distortion ratio in the message channels in the frequency multiplexed mastergroup of greater than 30 dB; the effect of high-frequency jitter is crosstalk between channels less than theoretical 9-digit quantizing noise.

In order to meet this objective with an economical repeater design, appropriately spaced high Q jitter reducers[7] are required along the line. A jitter reducer includes an automatic phase control (APC) loop to smooth the jittered timing wave, and buffer storage for the information pulses. The information pulses are read into the store by the jittered timing wave and read out by the smoothed wave.

The jitter performance required of each repeater is a function of the

* In Ref. 5, this objective was given for a coded U600 mastergroup in which the top frequency is 3.084 MHz.

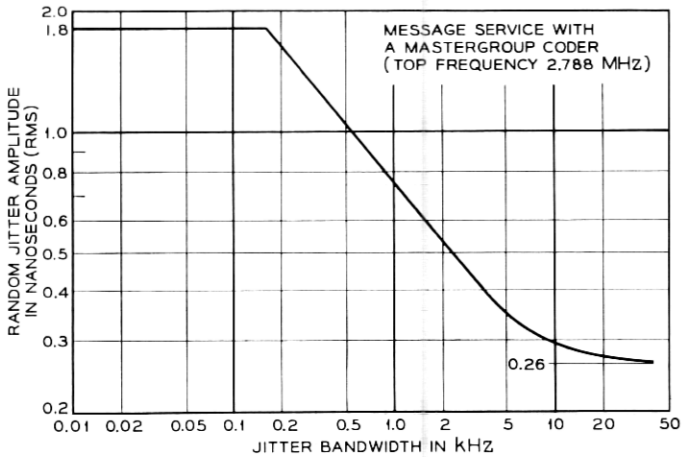

Fig. 18 — Objective for the maximum overall band-limited jitter due to random pulse sequences in a 4000-mile digital repeatered line.

overall jitter objective, the number of jitter reducers in the overall line, the effective Q of each of the jitter reducers, and the effective Q of the timing circuits in the repeaters.

The accumulation of jitter in a chain of repeaters with uniformly spaced jitter reducers can be analyzed by an extension of the technique developed for the analysis of jitter accumulation in the T1 system.[8,17] The analysis is based on a model in which the following assumptions are made:

(*i*) The significant jitter at the end of a chain of repeaters arises from the addition of the systematic, or pulse pattern dependent, jitter introduced in each repeater.

(*ii*) At the end of a long chain of repeaters, the accumulated jitter due to a random pattern is gaussian.

(*iii*) With respect to the transmission of accumulated jitter, the repeaters and jitter reducers may be replaced by the low-pass equivalents of their timing paths.

(*iv*) In each repeater, the effect of all sources of jitter due to random patterns is equivalent to the effect of a single, band-limited, white timing-noise source at the input to the equivalent low pass network.

(*v*) The timing noise introduced in the jitter reducers is negligible.

The model has successfully predicted experimental results for the T1 system,[8] and there is every indication that the same will be true for a high-speed repeatered line with jitter reducers. The model for the high-speed line is shown in Fig. 19. $F_R(s)$ and $F_J(s)$ are the low-pass equiva-

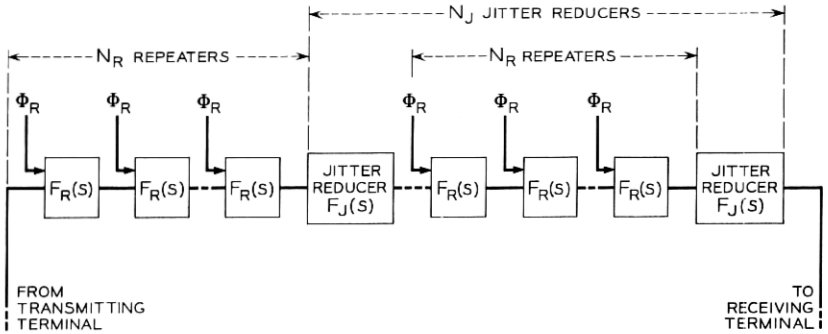

Fig. 19 — Model of a chain of repeaters and equally spaced jitter reducers for the analysis of the accumulation of jitter.

lents of the repeater and jitter reducer timing paths, and Φ_R is the power spectral density of the equivalent band-limited white timing noise source.

The results of an analysis are presented in Fig. 20 for a transcontinental system containing 3600 repeaters each with an effective Q of 80, and uniformly spaced jitter reducers each with an effective Q of 10^6. In this

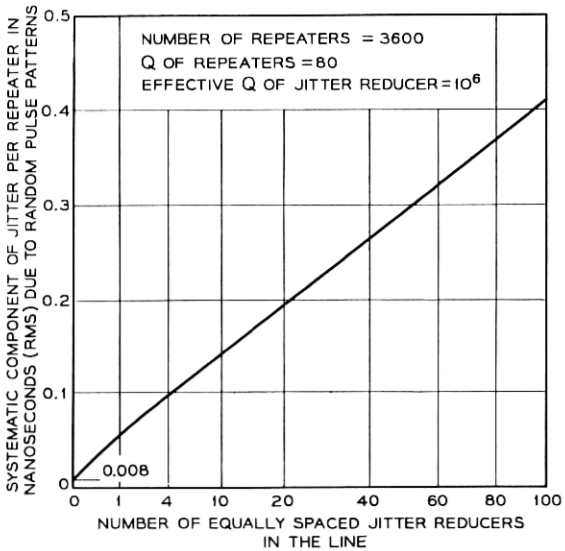

Fig. 20 — Objective for the systematic component of jitter (rms) contributed by a single repeater versus number of equally spaced jitter reducers.

figure, the requirement is given for the systematic component of jitter (rms) contributed by a single repeater due to random pulse patterns as a function of the number of equally spaced jitter reducers. If no jitter reducers were to be used, the repeater objective would be 0.008 ns rms or 0.6° rms, which when properly scaled is more stringent than the approximately 1° measured in T1.[8] Because of the higher-speed technology here, a practical requirement should be more liberal than the reported T1 performance. Based on our laboratory experience, a reasonable objective for the contribution of a single repeater to the systematic jitter due to random patterns is 0.1 ns rms or 8° rms. This leads to a need for four jitter reducers, each with a Q of 10^6, in 4000 miles, or one jitter reducer every 1000 miles. In an actual system, jitter reduction is required at all multiplex points. These occur, on the average, at intervals substantially smaller than 1000 miles, so that jitter reduction does not influence the main station spacing. Further, jitter reducers with Q's of less than 10^6 would be used.

IV. DESIGN OF THE REPEATER

A block diagram of the repeater is shown in Fig. 21. As briefly described in Section 2.1, the regenerative repeater performs the functions known as the three R's—reshaping, retiming, and regeneration. The

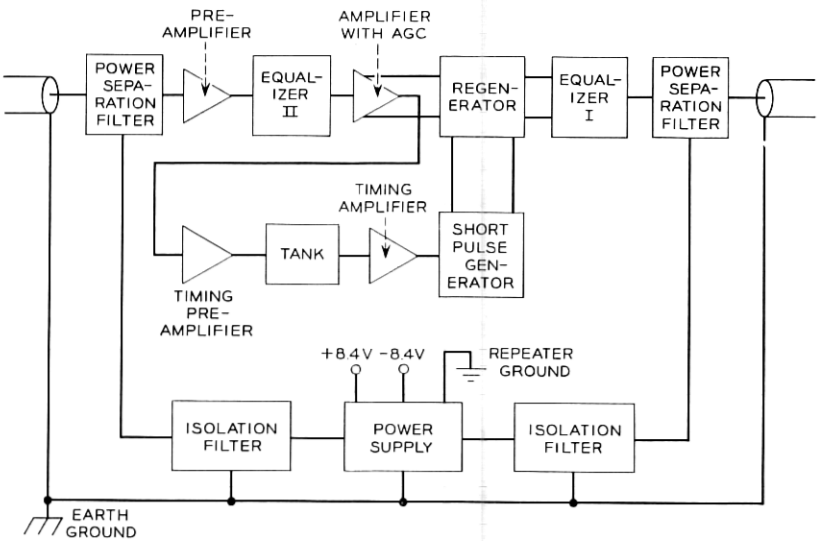

Fig. 21 — Functional block diagram of the repeater.

linear signal path (Fig. 10), comprising Equalizer I in the previous repeater, the preamplifier, Equalizer II, and the amplifier, reshapes and amplifies the pulse in preparation for detection. The timing path extracts a periodic timing wave from the signal train and generates a train of short sampling pulses occurring near the centers of the baud intervals, where the eye has its maximum opening. The regenerator provides crosshair pulse detection; at a time established by the sampling pulses, the signal pulse is compared with a threshold voltage, and if the threshold is exceeded, a new pulse is generated and transmitted to the next repeater. Since this is a ternary repeater, two such thresholds are provided. A second set of short periodic pulses controls the output signal pulse duration by turning off the regenerator after one-half baud interval.

The circuits shown on the block diagram of Fig. 21 were constructed on printed wiring boards and interconnected by sections of shielded transmission line on a printed interconnecting board. The development of the individual circuits was carried out independently between resistive terminations equal to the characteristic impedance of the transmission line used. Good cascading behavior was insured by controlling the forward transmission and the input impedance with load.

The complete repeater uses 25 transistors; 14 of these are a Bell System pnp germanium planar design with a cutoff frequency, f_T, of 4 GHz; 9 are a Bell System npn silicon design with an f_T of 1 GHz; and the remaining two are lower-frequency transistors of standard codes. A pair of gallium arsenide Esaki diodes provide the decision thresholds; a pair of charge storage diodes are used to generate the short sampling and turn-off pulses. Schottky barrier diodes are used in many circuits where high speed and low capacitance are required.

The description of the repeater circuits is organized into four sections: *reshaping* by the linear signal path, *retiming* by the timing path, *regeneration*, and *secondary features* such as powering and surge protection.

4.1 *Reshaping: The Linear Signal Path*

4.1.1 *Equalization*

The overall shape of the equalization is specified by the singularities indicated in Table II. Since the peak output power of the repeater is limited, minimum noise reaches the decision point in the regenerator if all of the passive equalization is placed beyond the preamplifier, a source of the noise. It is advantageous, however, to sacrifice a small amount of noise performance by placing a portion of the low-frequency attenu-

ating equalization ahead of the preamplifier to prevent its overload by certain pulse sequences strong in low-frequency content. With the PST code, the peak amplitude of the unequalized sequence varies over a 28-dB range, as stated earlier.

Once placed in front of the preamplifier, there is further advantage in placing this low frequency attenuating portion of the equalizer at the output of the previous repeater. This aids in protecting the regenerator against lightning and power surges, both rich in low frequencies relative to our band of interest.

The response characteristics and circuit configurations of Equalizers I and II are shown in Figs. 22 and 23. Equalizer I consists of a single

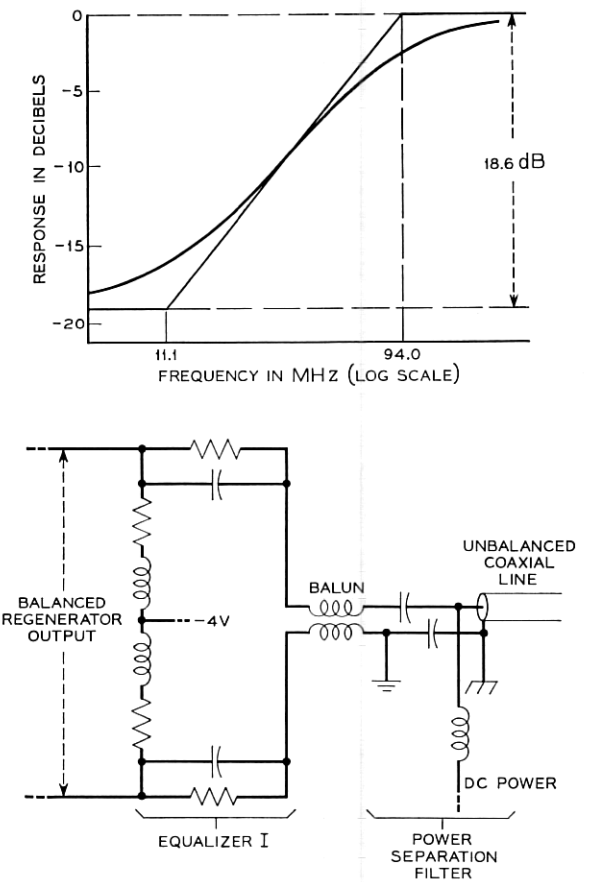

Fig. 22 — Equalizer I—attenuation characteristic and circuit configuration.

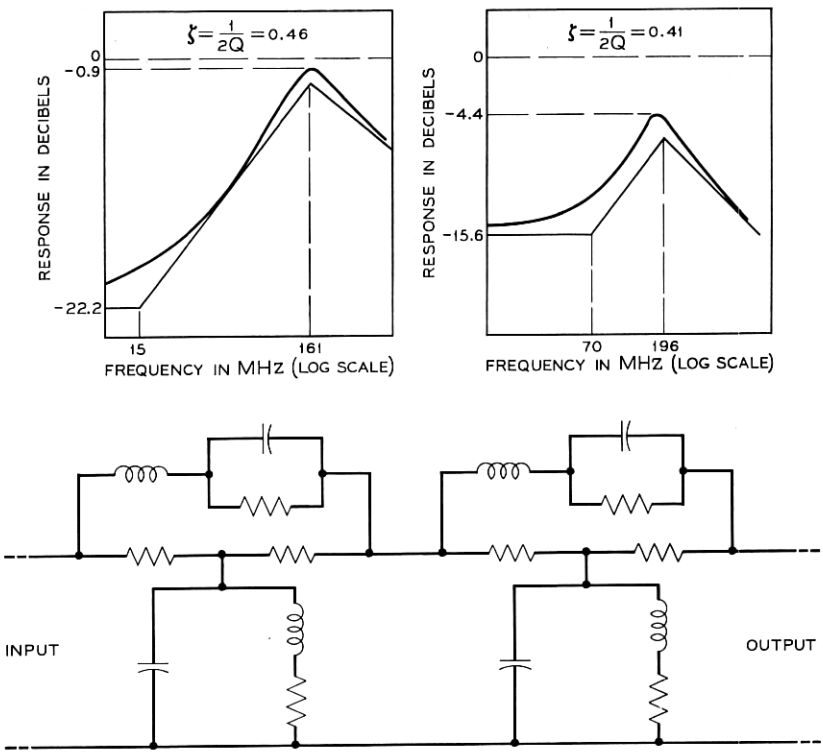

Fig. 23 — Equalizer II — attentuation characteristic and circuit configuration.

doublet with the zero at 11 MHz and the pole at 94 MHz. Notice the balanced nature of Equalizer I, which couples the balanced regenerator outputs to the unbalanced coaxial line through a balun and the unbalanced power separation filter.

Equalizer II comprises two constant R sections, each with a real zero and a complex pole pair. The first section has a zero at 15 MHz and poles at 161 MHz $\angle \pm 117°$ and the second section has a zero at 70 MHz and poles at 196 MHz $\angle \pm 114°$.

4.1.2 *Amplification*

It is the function of the preamplifier and amplifier to provide essentially flat gain while maintaining the desired equalized pulse shape. To accomplish this without complex delay equalization requires a bandwidth exceeding 300 MHz. The phase characteristic of this gain was

taken into account in the computer simulation that led to the equalization choice. A calculation of the gain required in the preamplifier and amplifier at 112 MHz is as follows:

Cable loss	57 dB
Equalization loss at 112 MHz relative to minimum loss	6 dB
Minimum loss of equalization	9 dB
Matching padding at amplifier input to achieve adequate return loss	6 dB
Nominal loss of variolosser (in amplifier for AGC)	5 dB
Effective ratio of amplifier to regenerator peak power outputs	−4 dB
Total gain required	79 dB

This gain is split with 26 dB in the preamplifier, and 53 dB in the amplifier.

The preamplifier curcuit, shown in Fig. 24, uses three transistors, each having a 4-GHz f_T, in common emitter configurations with collector to base feedback. The series diode gate at the input provides surge protection for the input transistor, and in the process loses 1 dB in noise figure and in gain. The overall circuit shown has a 6-dB noise figure at the frequencies of interest and a gain of 26 dB.

The amplifier functions (*i*) to terminate Equalizer II accurately in 50 ohms, (*ii*) to amplify the signal 48 dB nominally, with an AGC range of ±5 dB from nominal, (*iii*) to provide balanced outputs of 1 volt across each of the two regenerator 50 ohm inputs, and (*iv*) to rectify the bal-

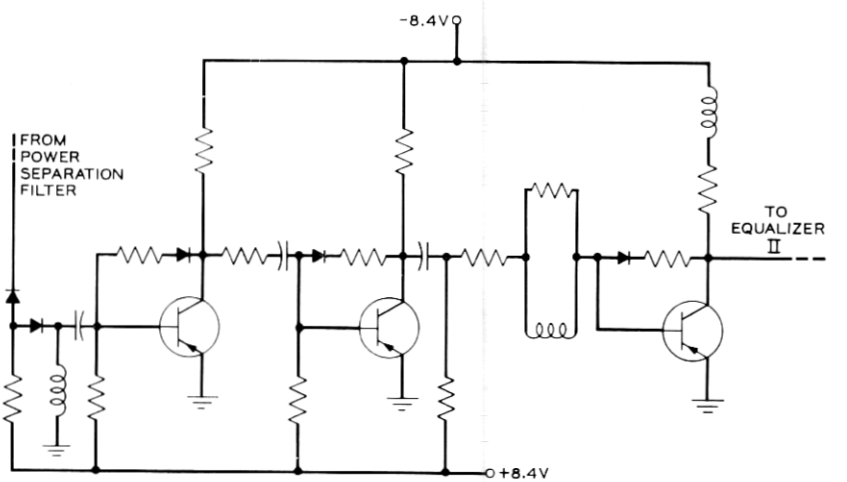

Fig. 24 — Preamplifier circuit.

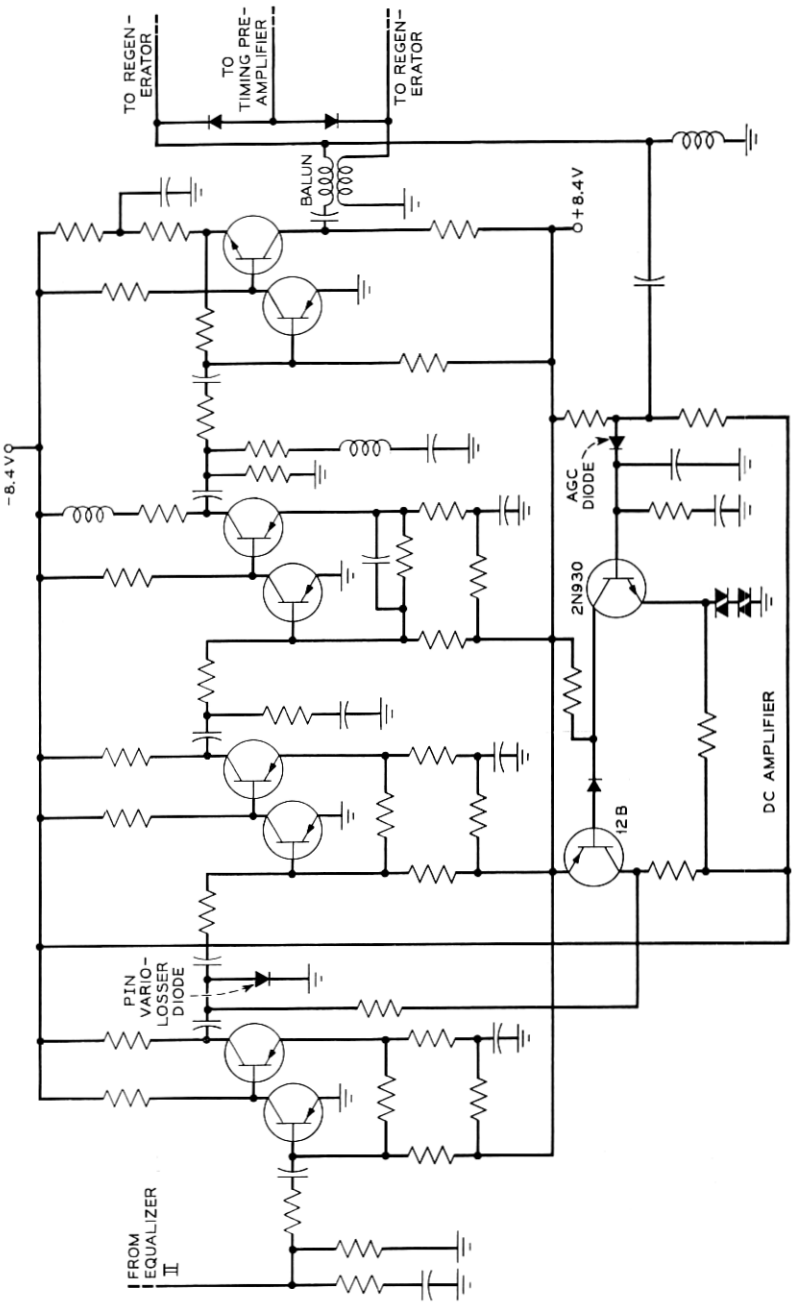

Fig. 25 — Amplifier circuit.

anced output to provide signals for the timing path. A circuit diagram of the amplifier is shown in Fig. 25. The basic gain stages are two-transistor doublets.[18] All transistors in the forward signal path are the 4-GHz pnp type, except the final transistor which is the 1-GHz npn type. The two transistors in the dc amplifier for the AGC are standard codes as noted.

The AGC diode compares the positive peak equalized signal amplitude with a reference derived from the power supply. When the amplitude is too large (small) the difference is amplified and the PIN variolosser diode current is increased (reduced). The advantage of a PIN diode over a pn-junction diode is that variolosser action is not obtained by the nonlinear conductance of a junction, but rather by the conductivity of the intrinsic region, determined by the dc control current. In this manner, currents of tenths of milliamperes are used to control signal power up to 1 milliwatt. The AGC loop gain is 40 dB at midrange.

4.2 *Retiming*

The timing path generates two trains of periodic subnanosecond pulses from information extracted from the equalized pulse stream. One train is for timing the decisions in the regenerator; the other, of opposite polarity, is for control of the duration of the regenerator output pulses. The relative phase between the sampling pulses and the information pulses at the regenerator input is determined by the timing path.

The timing path begins with the full-wave rectifier at the output of the amplifier (Fig. 25). The diodes are biased to transmit the upper 65 per cent of the rectified signals. This clipping level was shown to give best jitter performance both in an analog computer simulation of the timing path and in tests on the actual circuits. As indicated in Fig. 21, the clipped signal drives the timing preamplifier, which in turn drives a resonant tank tuned to the baud frequency. The output has pulse pattern dependent amplitude variations of approximately 14 dB; the $+0-0+0-\cdots$ sequence gives minimum amplitude and the $+-+-+-\cdots$ sequence gives maximum amplitude. This signal is amplified and limited to obtain a uniform high-amplitude sine wave, which in turn is coupled to a pair of oppositely poled charge storage diodes to generate the two required subnanosecond pulse trains.

4.2.1 *The Resonant Tank*

The tank is a loaded cavity with inductive loops for input and output coupling. The loaded Q is 80. An exploded view in Fig. 26(a) shows its

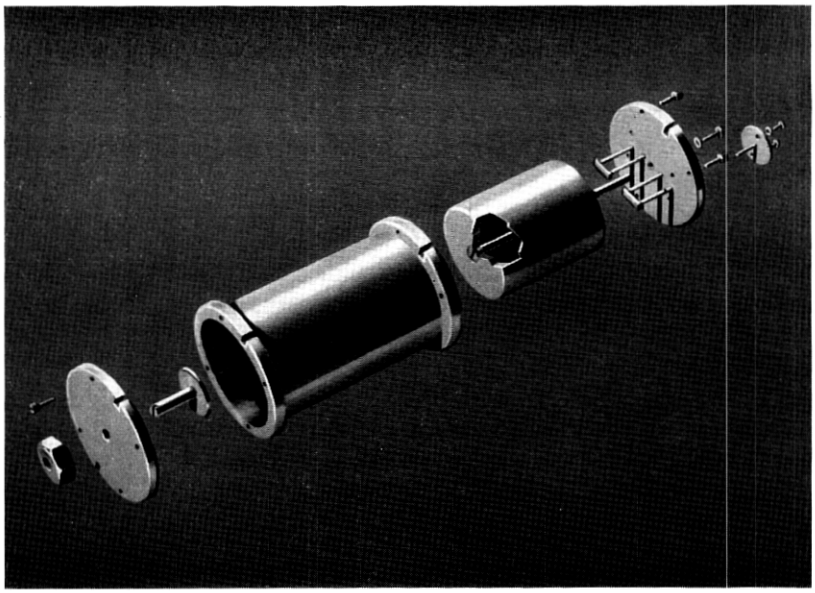

(a)

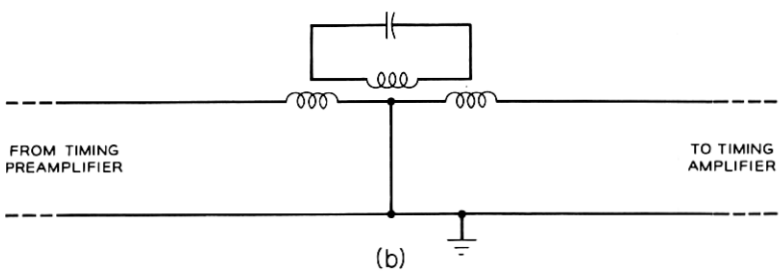

(b)

Fig. 26 — The resonant tank; (a) exploded view; (b) equivalent circuit.

construction, and the equivalent circuit in Fig. 26(b) shows its operation. The resonant frequency is stabilized with respect to temperature by the use of invar for the center post. This frequency can be adjusted over a narrow range by trimming the capacitance of the tank by adjusting the position of the disc attached to the trimming screw shown at the left end of Fig. 26(a).

We allow a maximum of ± 0.1 radian (5.7°) of static timing misalignment due to tank mistuning with age (20 years), and temperature (a range of 40°F). The phase shift, φ, of a high Q resonant circuit is

given for small values by

$$\varphi \approx 2Q \frac{\Delta f}{f}$$

where f is the resonant frequency and Δf is the mistuning. Hence, for a Q of 80, the tolerance on the resonant frequency is

$$\frac{\Delta f}{f} = \frac{\pm 0.1}{160} \quad \text{or} \quad \pm 0.0625\,\%$$

This level of performance is attained with the machined structure of Fig. 26, provided that it is operated between well-controlled impedances.

4.2.2 *Amplification in the Timing Path*

For the pulse sequence with maximum timing energy, the baud frequency component of the rectified timing signal has a peak amplitude of 150 mV. For the sequence with minimum energy, this component is 30 mV, or 14 dB lower. The peak amplitude of the required timing amplifier output is 3 volts, or 40 dB above 30 mV. In addition, as will be shown in Section 4.2.3, a minimum of 8 dB of limiting for the lowest level signal is required for good performance. Further, the tank has a loss of 0.5 dB at the baud frequency. Thus, linear gain of 40 + 8 + 0.5 = 48.5 dB is required in the timing path.

The 3-stage timing preamplifier, shown in Fig. 27, provides 22.5 dB of gain, and the 5-stage timing amplifier, shown in Fig. 28, provides 26

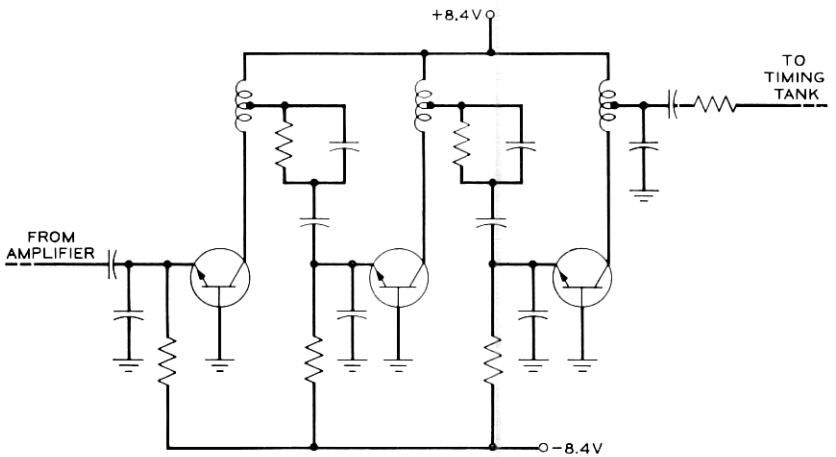

Fig. 27 — Timing preamplifier circuit.

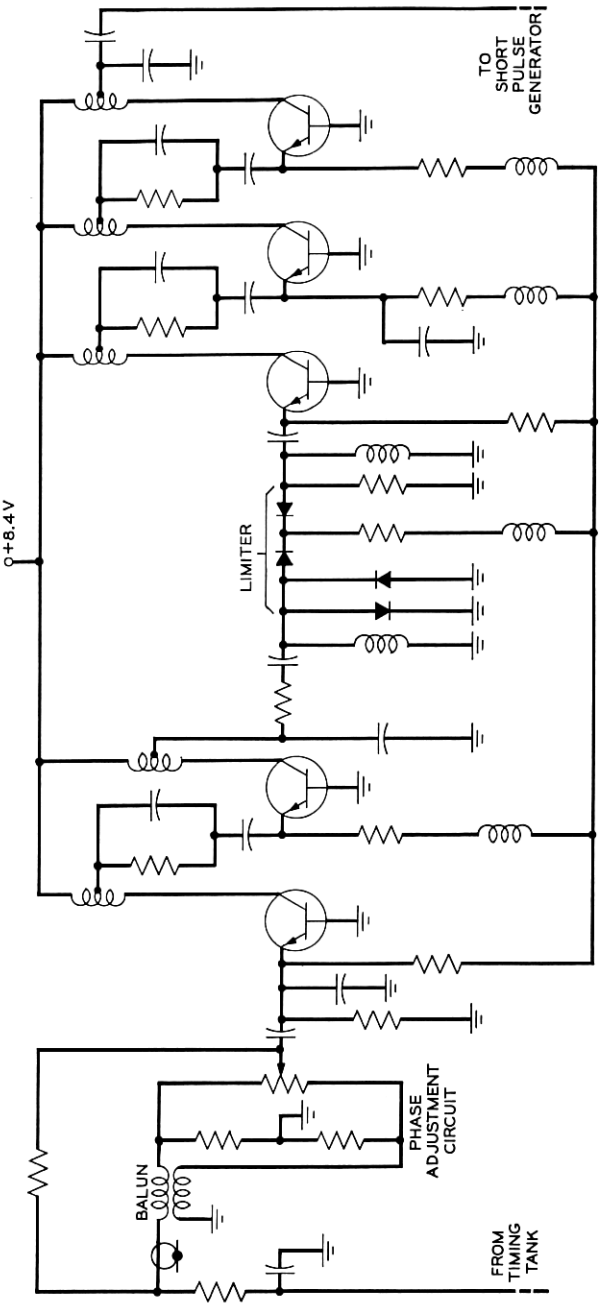

Fig. 28 — Timing amplifier circuit.

dB of gain at levels low enough not to produce limiting. Each stage has about 8 dB of gain, but the amplifier includes a phase adjustment circuit with 13 dB of loss, as described in Section 4.2.4. Both amplifiers employ common base stages coupled by bifilar-wound transmission line auto-transformers to provide current gain. All eight transistors are the 1-GHz npn silicon type.

As indicated in the composite frequency response of Fig. 29, the bandwidths of the timing path amplifiers are quite broad. This broadband design reduces the sensitivity of the timing path phase response to variations in amplifier reactive elements with age and temperature.

4.2.3 *Limiting*

A series gate employing Schottky barrier diodes at the output of the second stage of the amplifier is used to perform limiting, as shown on Fig. 28. Transistor limiting was avoided in order to keep amplitude-to-phase conversion at a minimum. The main cause of amplitude-to-phase conversion in this series type of limiter comes from diode shunt capacitance. With very large signals, significant reactive current flows through this capacitance and advances the phase of the output wave. This effect is kept small by the use of the shunt diodes to reduce the voltages reaching the series diodes. The amplitude-to-phase conversion of the limiter for the 7-mA diode current used is shown in Fig. 30(a).

Since the phases of the pulse trains generated by the charge storage diodes are heavily dependent upon the sine wave amplitude, the flatness of limiting shown in Fig. 30(b) is also important. Notice that an input of 0.35 volts at the lower end of the 17-dB range results in an output of

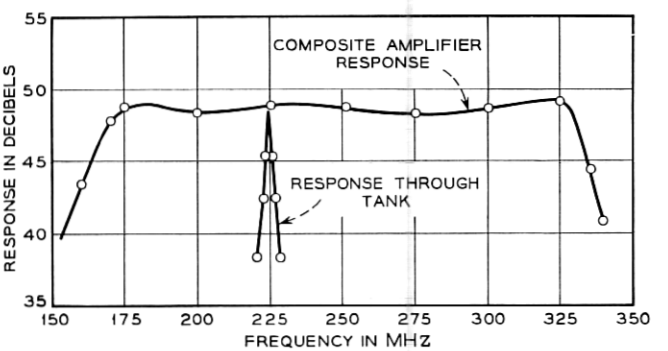

Fig. 29 — Composite frequency response of the timing path amplifiers.

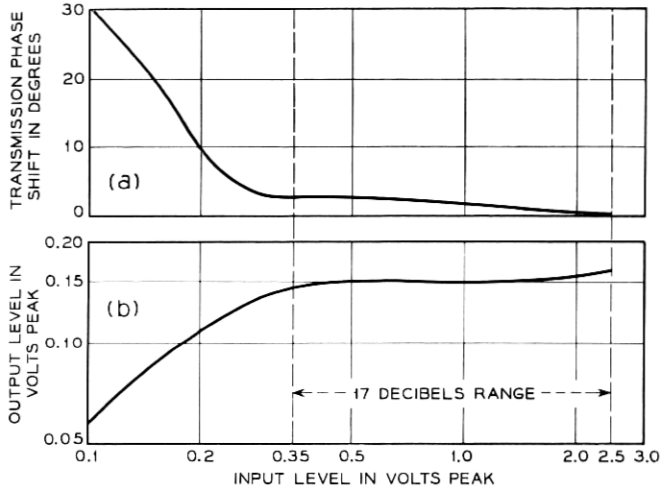

Fig. 30 — Limiter performance; (a) transmission phase shift vs input signal; (b) output signal vs input signal.

0.14 volts. This corresponds to the 8 dB of minimum limiting referred to earlier. The 17-dB range is the sum of 14 dB due to timing wave amplitude variations and 3 dB due to loss variations in the phase adjustment circuit to be described next.

4.2.4 *Phase Adjustment Circuit*

In order to set the sampling pulse at the center of the eye, a phase adjustment is required in the timing path. The circuit at the input to the timing amplifier (Fig. 28) was designed to permit a $\pm 45°$ adjustment range on the phase of the timing wave. The coaxial transmission line provides 90° of phase shift between the input and the upper end of the potentiometer. Due to the balun, there is 180° phase difference between the upper and lower ends. Two currents are summed at the emitter of the first amplifier stage. One current, I_R, at reference phase in the vector diagram of Fig. 31, comes directly from the input; a quadrature current, I_Q, comes from the movable tap. By moving the tap upward in the diagram, more phase lag is introduced and vice-versa. Over the extreme range of the potentiometer, for which I_Q is indicated by the dashed lines, 3 dB of amplitude variation is introduced, an amount which the limiter removes.

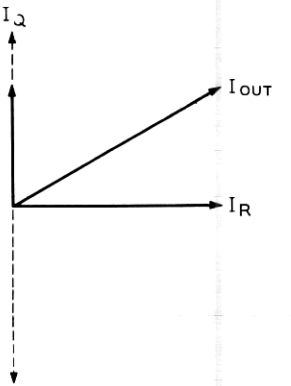

Fig. 31 — Vector diagram for phase adjustment circuit.

4.2.5 *The Short-Pulse Generator*

The circuit to generate the subnanosecond sampling and turn-off pulses is shown in Fig. 32. A sine wave of current from the timing amplifiers flows through the diode in the forward direction, storing charge. During this portion of the operation, the rather small forward voltage drop appears across the diode. When the sinusoidal current reverses polarity, the stored charge permits reverse conduction until the charge is depleted, whereupon the diode current abruptly falls to zero.[19,20] The feed inductor current is abruptly switched from the diode to the load to produce a rapid rise of current. The decay transient determining the short pulse duration is established by the coupling network with the diode open-circuited.

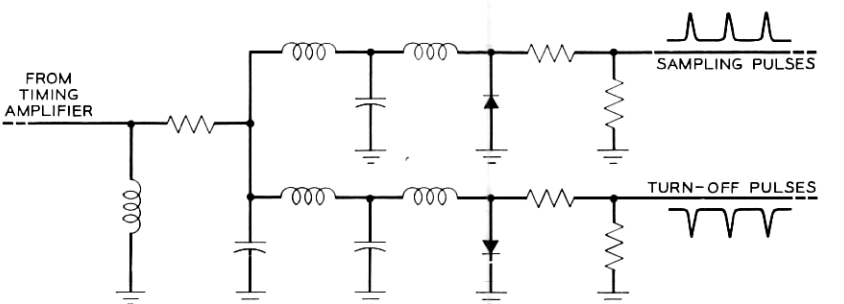

Fig. 32 — Short-pulse generator circuit.

4.3 *Regeneration*

In the regenerator, the ternary signal requires two amplitude thresholds, which are obtained by providing two identical decision circuits driven with oppositely phased signals from the balanced amplifier output. Each decision circuit incorporates a two-input AND gate and an Esaki diode, shown as part of Fig. 33. The signal is applied to one input of the gate and subnanosecond sampling pulses to the other. With a positive signal pulse present, the sampling pulse diverts the AND gate current from the sampling pulse diode to the AND gate output, where the Esaki diode is triggered to its high-voltage state. With either a zero or negative input signal, the gate current flows toward the signal source, and the Esaki diode remains untriggered. A subnanosecond negative turn-off pulse, one-half baud interval after the sampling pulse, returns the Esaki diode to its low-voltage state, establishing the repeater output pulse duration of 2.2 nanoseconds.

The Esaki diode voltages of the two decision circuits are amplified in a pair of current routing output stages, employing the 4-GHz germanium transistors. The resulting balanced outputs of these stages are combined to give the appropriate signal polarities at the repeater output.

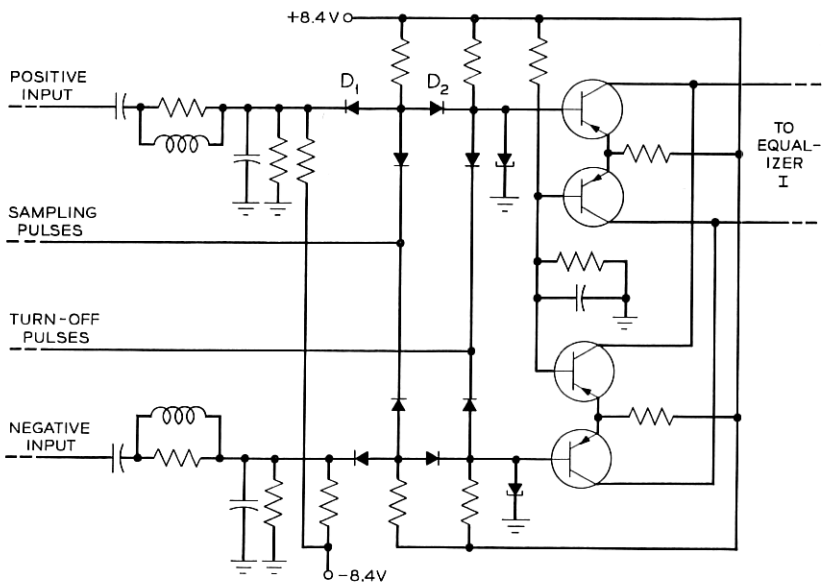

Fig. 33 — Regenerator circuit.

4.3.1 *Input Networks*

The inputs to the regenerator are ac coupled. The shunt capacitors (Fig. 33) reduce timing energy coupling onto the input signal leads. Since the timing path begins at the amplifier output, such coupling feeds energy back into the timing path, thereby increasing pattern dependent jitter. The other elements of the input networks provide good 50-ohm terminations for the amplifier signals.

4.3.2 *The Threshold Circuits*

A biasing circuit fixes the dc level of the signal relative to the threshold voltage, which is established by the Esaki diode. This threshold voltage and the signal bias are related through the back-to-back diodes of the AND gate to provide temperature tracking. The signal bias is chosen to place the Esaki diode threshold *voltage* at the center of the eye.

A discussion of the operation of the threshold circuit follows. At the threshold of triggering the Esaki diode, with the sampling pulse present, equal current flows through diodes D_1 and D_2 of the AND gate. It can be shown that this condition corresponds to maximum signal transmission, which provides maximum regenerator sensitivity.

An applicable model of the Esaki diode and its sources, shown in Fig. 34(a), is the parallel combination of a signal current source, I_S, a bias current source, I_B, a linear source resistance, a capacitance, and a nonlinear resistance whose static characteristic is shown in Fig. 34(b). The difference between the load line current and the static characteristic current is capacitive current I_C of our model. Threshold voltage V_A is the voltage at point A, the unstable intersection of the load line and the diode static characteristic. Initially, the voltage is V_C, the low voltage state. The subnanosecond sampled signal pulse charges the capacitance, raising the voltage. If after this pulse has passed, the resulting voltage is greater than V_A, excess current is available to further charge the capacitance, stable point B will be reached, and the decision will be that a pulse was present. If the voltage is less than V_A, the capacitance will discharge, operation will return to point C, and the decision will be that no pulse was present.

For good dynamic performance — that is, high circuit speed at the threshold level — the load line should intersect the diode negative resistance at a steep part. For high circuit gain, on the other hand, the load line should be raised toward the peak so that smaller AND gate current can be used (the amplifier must supply a peak-to-peak signal current equal to the gate current) and larger voltage can be obtained to

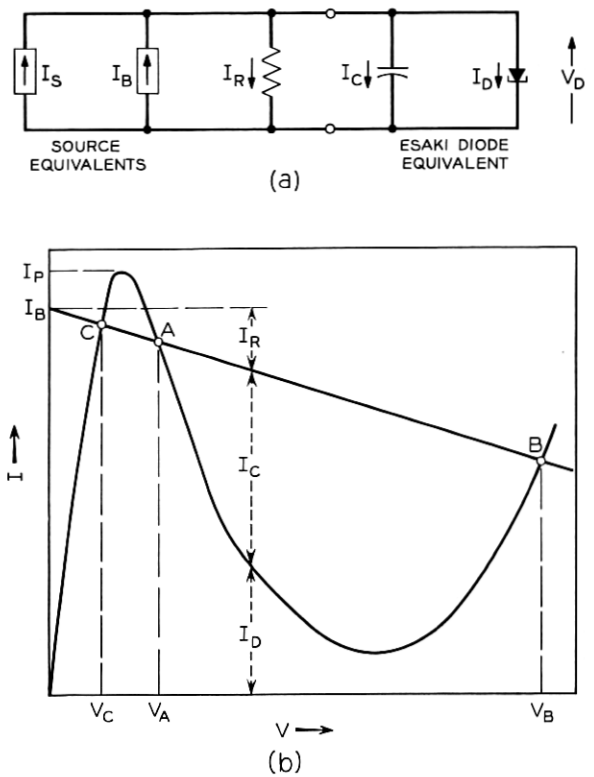

Fig. 34 — Esaki diode model; (a) equivalent circuit; (b) volt-ampere characteristic of nonlinear resistance.

drive the current routing stages. Further, for stability against changes in diode peak current with age and temperature, biasing current I_B should be small and the gate current should be large. As a suitable compromise among these factors, a bias current of 8 mA and a gate current of 4.5 mA were chosen in conjunction with a gallium arsenide Esaki diode having a peak current, I_P, of 10 mA.

The input-output dynamic regenerator characteristic was calculated using the equivalent circuit of Fig. 34(a) and a piece-wise linear approximation to the diode characteristic of Fig. 34(b). The performance was measured for six regenerators in the experimental setup of Fig. 35(a). A comparison of the limits of the measured characteristics and the calculated characteristic is shown in Fig. 35(b). It was indicated in Section 3.2.2 that the total area and not the amplitude of the regenerator output pulse primarily controls the amplitude of the pulse arriving at the sub-

sequent regenerator after transmission and equalization. Hence, the use of the simulated equalized line for $T(f)$ permits the proper comparison of equalized amplitudes, V_{out}.

4.3.3 *Output Amplifiers*

The emitter-coupled current routing pair of Fig. 33, which amplifies the Esaki diode voltage, has five important features. First, the circuit is fast because of the prevention of saturation. Second, it performs the inversion required for the negative pulse decision circuit. Third, its nonlinear forward transmission characteristic provides additional amplitude regeneration. Fourth, it has good dc temperature stability due

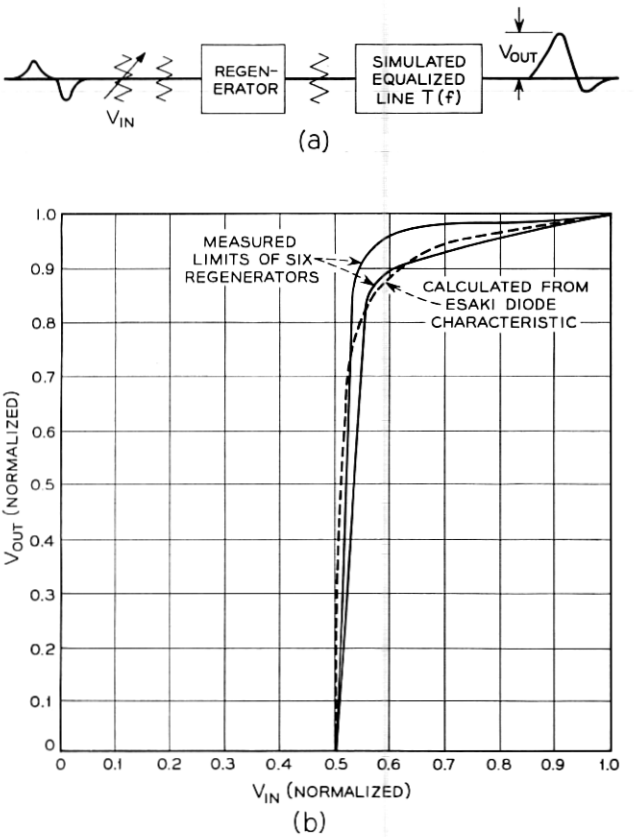

Fig. 35 — Input-output dynamic regenerator characteristic; (a) experimental setup; (b) measured and calculated characteristic.

to the oppositely poled emitter junctions between the signal and the reference inputs. (The Esaki diode signal voltage is a unipolar pulse stream which includes a dc component.) Fifth, to a first approximation, signal currents flow equally and oppositely in the two output leads and thus no current from the output flows through the ground system of the repeater. Many kinds of repeaters powered serially over the transmission line suffer from feedback problems due to such currents.

The output collectors of the two current-routing circuits are paralleled into balanced 75-ohm loads, to which they deliver peak output voltages of 1.5 volts of each polarity.

4.4 *Secondary Features*

4.4.1 *Power Arrangement*

Repeaters are powered serially by dc over the center conductor of the coaxial. The line current is 450 mA. Power supply voltages in the repeater are obtained by passing about 50 mA of this current through a series pair of 8.4-volt Zener diodes as shown in Fig. 36. Thus, each repeater consumes 7.5 watts.

In Fig. 36, we show only the circuit elements required to separate the dc power from the signal. Feedback from output to input is attenuated

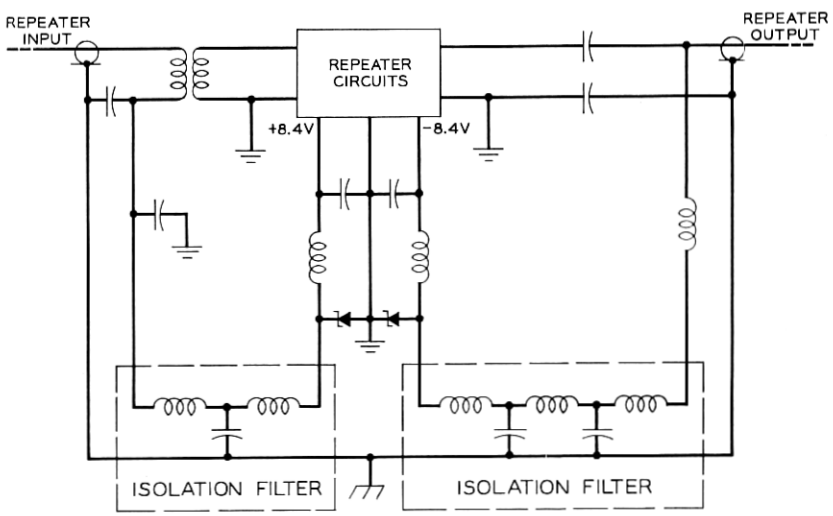

Fig. 36 — Repeater powering circuit.

in the power circuits by greater than 130 dB over the signal frequency range.

It is difficult to prevent spurious signals from appearing between earth ground and local repeater ground. In a long system, these two grounds may differ by as much as 1000 volts dc and capacitors with adequate voltage rating have appreciable impedance at frequencies of interest. Filtering inductors are required to prevent these ground-to-ground voltages from affecting the sensitive repeater circuits. The philosophy here is to isolate the repeater circuits from earth ground as much as possible.

4.4.2 *Surge Protection*

Partial surge protection has been provided at both the input and the output of the repeater. At the input, a series diode gate (Fig. 24), with 4 mA of current through each diode, limits the surge at the base of the first transistor. At the output, Equalizer I reduces the low frequency power which could harm the transistor collectors. These surge protection features are laboratory precautions only. Complete protection against lightning and power surges has not been accomplished in this experimental repeater.

4.4.3 *Repeater Equipment Design*

The repeater circuits shown on Fig. 21 were constructed on printed wiring boards which plug into a 3-layer printed wiring interconnecting board. The plug-in boards are attached to aluminum backing plates which provide support and an electrical ground plane for the circuits. The plates slide into the grooved sides of pockets in an aluminum investment casting. Fig. 37 is a photograph of a repeater showing the circuit boards in place in the casting, except for the amplifier board which has been removed. Shielding covers have been removed and are not shown.

Printed wiring carries shielded dc power to the individual circuit boards from the power supply on the interconnecting board (at the back of the casting in the photograph). Signal interconnections are made by miniature coaxial transmission lines to provide shielding.

Tantalum thin-film integrated techniques were considered for the circuits of the repeater, and there appear to be no fundamental obstacles to their use. A thin film version of the preamplifier was built and performance was equal to or better than the printed wiring version.

The size of this repeater is approximately 4x5x11 inches for a volume

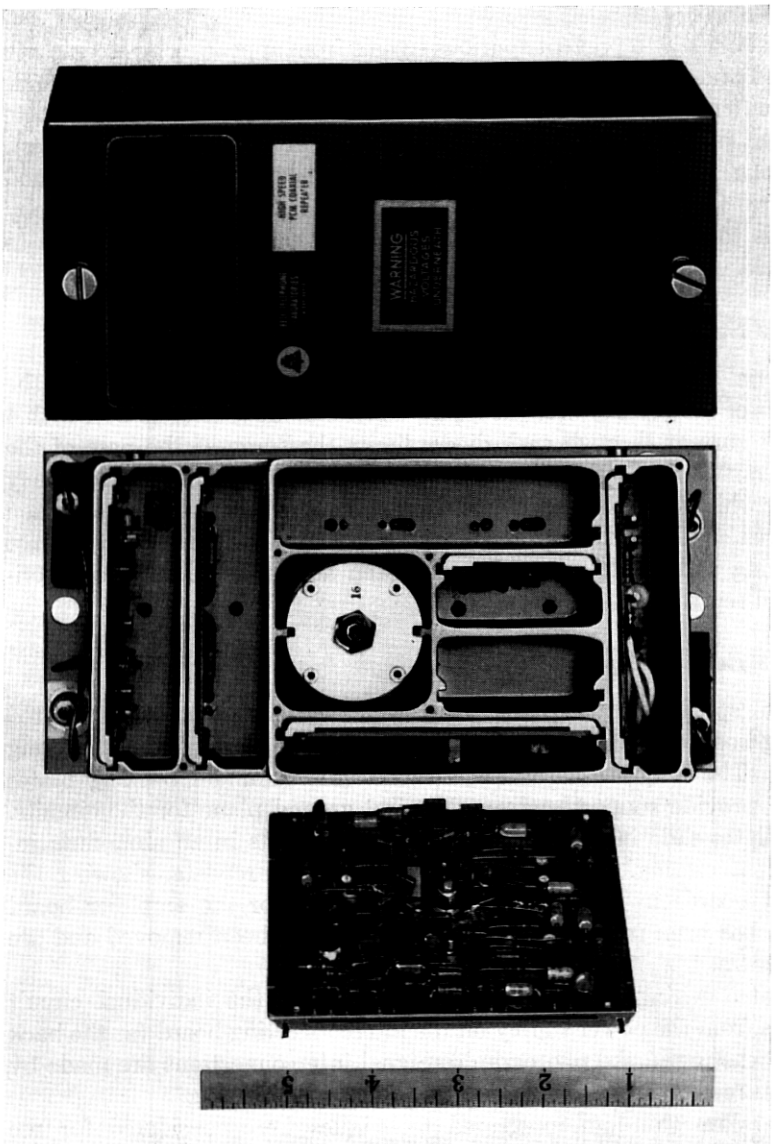

Fig. 37—Photograph of repeater with the amplifier printed circuit board removed. Shielding covers have been removed and are not shown.

of 220 cubic inches. By design, there is access space for testing of the experimental repeaters. It is anticipated that the use of integrated circuits and the elimination of excess space will result in a design occupying about one-quarter of the volume.

V. EXPERIMENTAL PERFORMANCE

In this section, we report on the performance of the line under laboratory conditions. In general, the line has met all performance expectations under these conditions. For volume manufacture, however, and for operation under field conditions for many years, further development is required. By the work reported on here, we have established the technical feasibility upon which a design for service can be based.

5.1 *Error Rate*

The line operates at error rates below 10^{-10} errors per baud through ten repeatered links.

5.2 *Jitter*

According to our model, each repeatered link introduces a pattern dependent, or systematic, component of jitter which is dominant. Pattern independent jitter tends to be random at each repeater; hence, it accumulates much more slowly and is negligible at the end of a long chain.

Since pattern dependent and pattern independent jitter are indistinguishable by measurement of a single link, we measure the jitter at the end of the chain. To determine the systematic component for the single link, we apply an equation derived from the model:[8]

$$\theta_1 = \sqrt{\frac{P(1)}{P(N)}}\,\theta_N$$

where θ_1 is the systematic rms jitter arising in each link, θ_N is the systematic rms jitter at the end of N links, and $P(N)$ is given by

$$P(N) = \frac{N}{2} - \frac{(2N-1)!}{4^N[(N-1)!]^2}$$

This function is tabulated in Ref. 8. For ten links, the above expression becomes

$$\theta_1 = 0.247\ \theta_{10}\,.$$

For only ten repeaters, the nonsystematic component may not be negligible, so that this calculation gives only an approximation to the systematic jitter contribution per link.

The total measured jitter at the end of our ten links is 13.3° rms. If we assume this to be all systematic, we calculate a per-link systematic jitter contribution of 3.3° rms. This laboratory measurement is well within the 8° objective of Section 3.3.2.

Fig. 38 shows the measured accumulated jitter versus the number of repeatered links. The intercept ($N = 0$) accounts for jitter introduced in the transmitting and receiving repeaters at the ends of the line.

5.3 *Waveforms*

In Fig. 39 we show some of the key waveforms in the repeater. All the waveforms are aligned in time for clarity. Fig. 39(a) shows the regenerator output before Equalizer I; 39(b), the signal input to the positive decision threshold of the regenerator; 39(c), the eye at this point when the line is driven by a random binary sequence; and 39(d), the subnanosecond sampling and turn-off pulses. For instructional purposes, the eye diagram has been synchronized at an even submultiple of the baud frequency to show the paired nature of the PST signal. The timing extractor causes the distortion in the negative eye. This distortion is of no consequence since only the positive eye is used by the positive threshold.

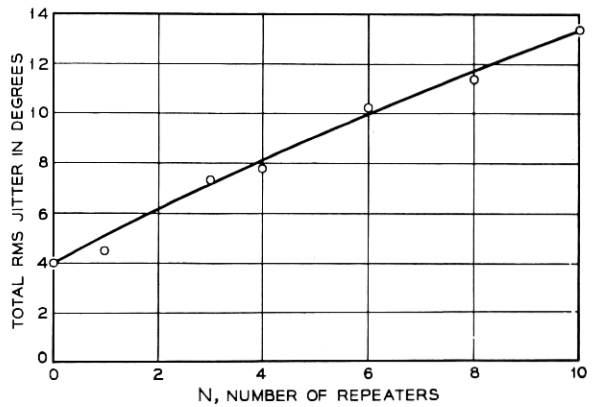

Fig. 38 — Measured accumulated jitter (rms) vs the number of repeatered links in the experimental line.

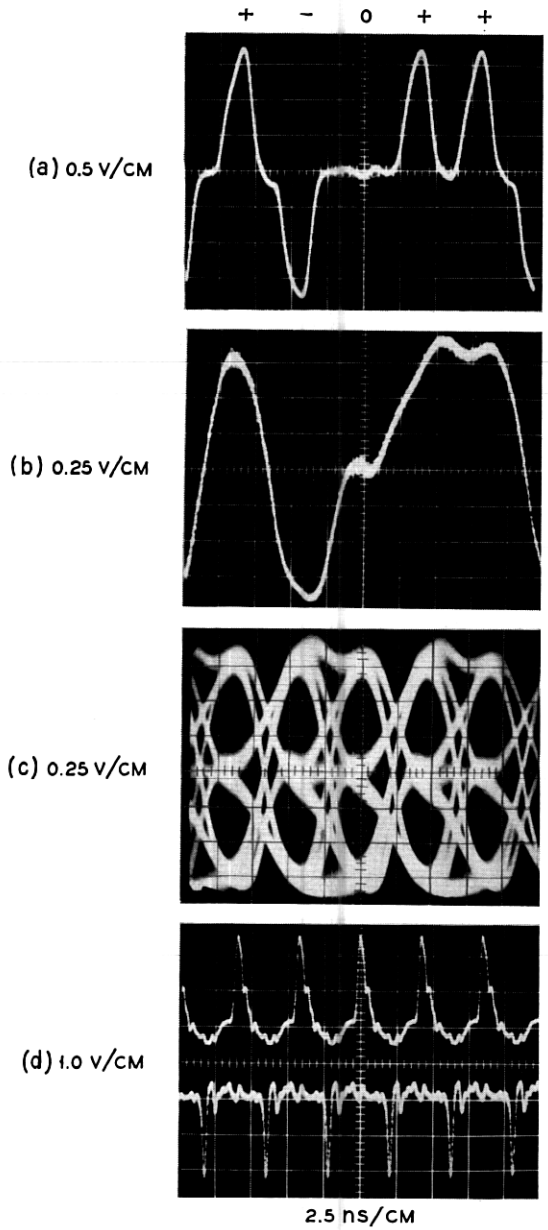

Fig. 39 — Key waveforms in the repeater; (a) regenerator output before Equalizer I; (b) signal input to the positive decision threshold; (c) the eye at the positive decision threshold; (d) the subnanosecond sampling and turn-off pulses.

VI. CONCLUSION

Ten 224-Mb/s experimental digital repeaters and associated code translation equipment have been developed, constructed, and operated over 10 miles of 0.270-inch coaxial line under laboratory conditions. The resulting performance has indicated that such a line 4000 miles in length is feasible for actual service and can be designed with existing techniques.

The transmission code is paired selected ternary (PST) which provides the essential features for the repeater operation as well as for in-service error monitoring.

Each repeater employs 25 transistors, most of them of a pnp germanium planar epitaxial design with an f_T of 4 GHz. The decision elements are gallium arsenide Esaki diodes.

The repeaters are serially powered by dc over the line with 450 mA of current, and each repeater consumes 7.5 watts.

Good agreement among theory, simulation, and laboratory performance has been achieved throughout. The error rate per repeatered link under laboratory conditions is less than 10^{-11} and the systematic jitter introduced in each link is about 3° rms.

VII. ACKNOWLEDGMENT

The work reported on herein was performed over a period of several years primarily by the members of the PCM repeater department under supervision of the authors. Many individuals have made significant contributions, but specific mention of these is not practical here. Prior work under the supervision of R. V. Sperry is gratefully acknowledged. The experimental cable was designed and manufactured through the efforts of Bell Laboratories' Outside Plant Laboratory, and Western Electric Company's Engineering Research Center and Baltimore Works. Support is also appreciated from many other departments within Bell Laboratories that have made contributions in areas such as systems engineering, components, devices, networks, and power. The work is based on earlier efforts over many years in the research department.

REFERENCES

1. Oliver, B. M., Pierce, J. R., and Shannon, C. E., The Philosophy of PCM, Proc. IRE, *36*, November, 1948, pp. 1324–1331.
2. Davis, C. G., An Experimental Pulse Code Modulation System for Short Haul Trunks, B.S.T.J., *41*, January, 1962, pp. 1–24.
3. Fultz, K. E. and Penick, D. B., The T1 Carrier System, B.S.T.J., *44*, September, 1965, pp. 1405–1451.
4. Travis, L. F. and Yaeger, R. E., Wideband Data on T1 Carrier, B.S.T.J., *44*, October, 1965, pp. 1567–1604.

5. Mayo, J. S., Experimental 224 Mb/s PCM Terminals, B.S.T.J., *44,* November, 1965, pp. 1813–1841.
6. Edson, J. O. and Henning, H. H., Broadband Codecs for an Experimental 224 Mb/s PCM Terminal, B.S.T.J., *44,* November, 1965, pp. 1887–1940.
7. Witt, F. J., An Experimental 224 Mb/s Digital Multiplexer Using Pulse Stuffing Synchronization, B.S.T.J., *44,* November, 1965, pp. 1843–1886.
8. Byrne, C. J., Karafin, B. J., and Robinson, D. B., Jr., Systematic Jitter in a Chain of Digital Regenerators, B.S.T.J., *42,* November, 1963, pp. 2679–2714.
9. Sipress, J. M., A New Class of Selected Ternary Pulse Transmission Plans for Digital Transmission Lines, IEEE Trans. Com. Tech., *Com-13,* September, 1965, pp. 366-372.
10. Elmendorf, C. H., et al., The L3 Coaxial System, B.S.T.J., *32,* July, 1953, pp. 781–1005.
11. Aaron, M. R., PCM Transmission in the Exchange Plant, B.S.T.J., *41,* January, 1962, pp. 99–141.
12. Ross, W. L., Private Communication.
13. Aaron, M. R. and Tufts, D. W., Intersymbol Interference and Error Probability, IEEE Trans. Inform. Theor., *IT-12,* January, 1966, pp. 26–34.
14. Smith, J. W., The Joint Optimization of Transmitted Signal and Receiving Filter for Data Transmission Systems, B.S.T.J., *44,* December, 1965, pp. 2363–2392.
15. Bennett, W. R., Methods of Solving Noise Problems, Proc. IRE, *44,* May, 1956, pp. 609–638.
16. Cravis, H. and Crater, T. V., Engineering of T1 Carrier System Repeatered Lines, B.S.T.J., *42,* March, 1963, p. 436.
17. Chapman, R. C., Private Communication.
18. Waldhauer, F. D., Wideband Feedback Amplifiers, IRE Trans. Circuit Theor., *CT-4,* September, 1957, pp. 178–190.
19. Goodall, W. M. and Dietrich, A. F., Fractional Millimicrosecond Electrical Stroboscope, Proc. IRE, *48,* September, 1960, pp. 1591–1594.
20 Moll, J. L., Krakauer, S., and Shen, R., *P-N* Junction Charge-Storage Diodes, Proc. IRE, *50,* January, 1962, pp. 43–53.